Advanced Transmission Electron Microscopy

Robin Schäublin

Ecole Polytechnique Fédérale de Lausanne
Centre of Reseach in Plasma Physics
Fusion Technology - Materials Group
Villigen PSI, Switzerland

A. Prokhodtseva, P. Unifantowicz, N. Baluc CRPP / C. Hébert, G. Lucas CIME EPFL/ E. Müller EMEZ ETHZ / T. Plocinski WUT / V. de Castro U. Carlos III / U. Oxford / D. Terentyev SCK·CEN / E. Meslin CEA Saclay / B. Décamps, O. Kaïtasov CNRS Orsay / A. Ramar CEN DTU

Introduction

Irradiation dose on the plasma facing components of the future fusion reactor is *high*:

- Fission reactor: ~1 displacement per atom [dpa] per year (Gen. I), 300°C
- Fusion reactor: ~30 dpa per year (DEMO), 800°C ?
- Radiation induced damage lead to hardening and embrittlement

One key to the fusion reactor is materials: first wall, divertor

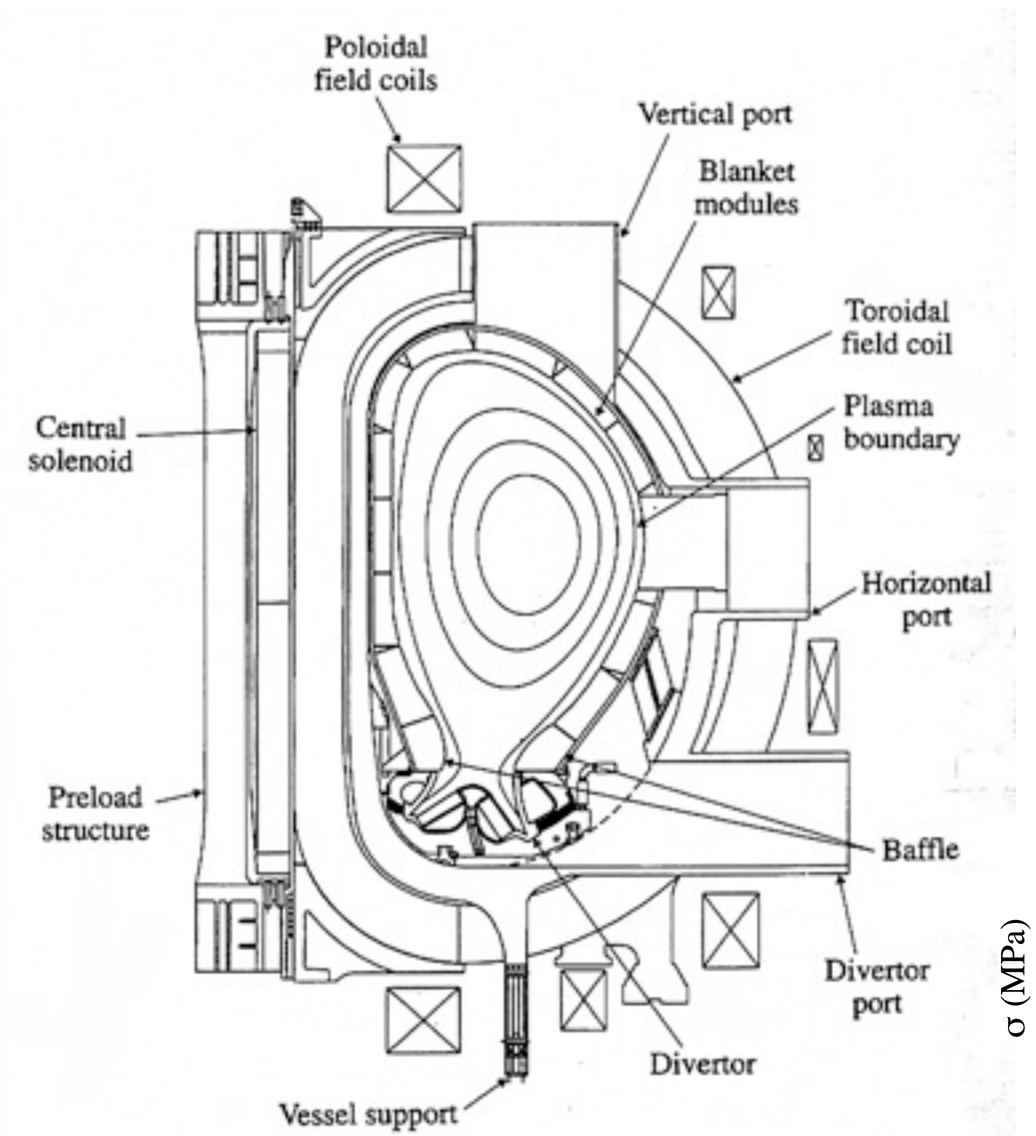

R. Schaeublin, D. Gelles, M. Victoria
J. of Nuclear Materials 307–311 (2002) 197–202

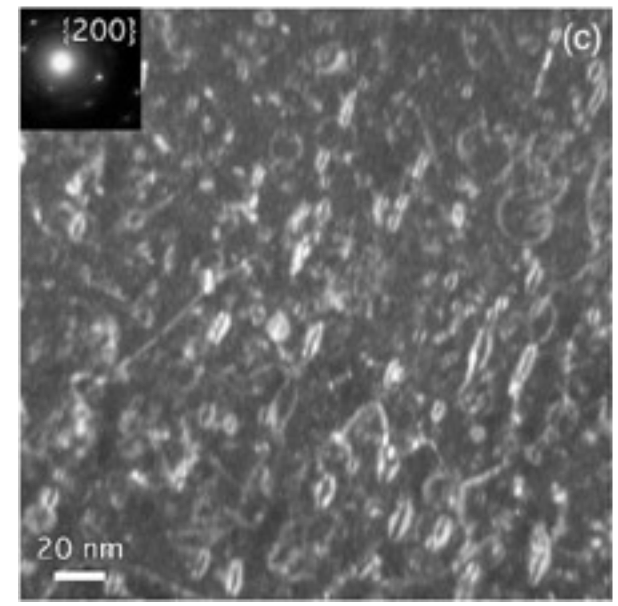

F82H
8.8 dpa 300°C

TEM picture

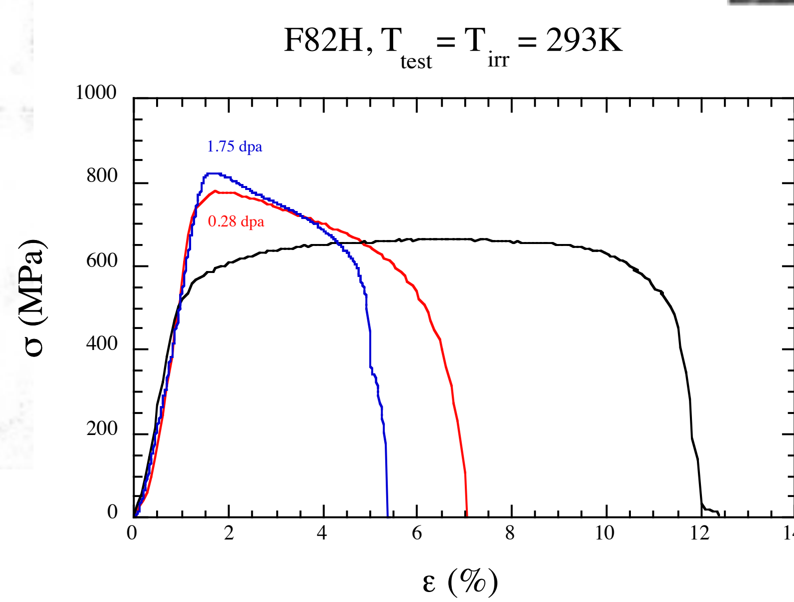

- hardening starting at the lowest doses

P. Spätig, R. Schäublin, et al.
Journal of Nuclear Materials, 258-263 (1998) 1345-1349

Introduction

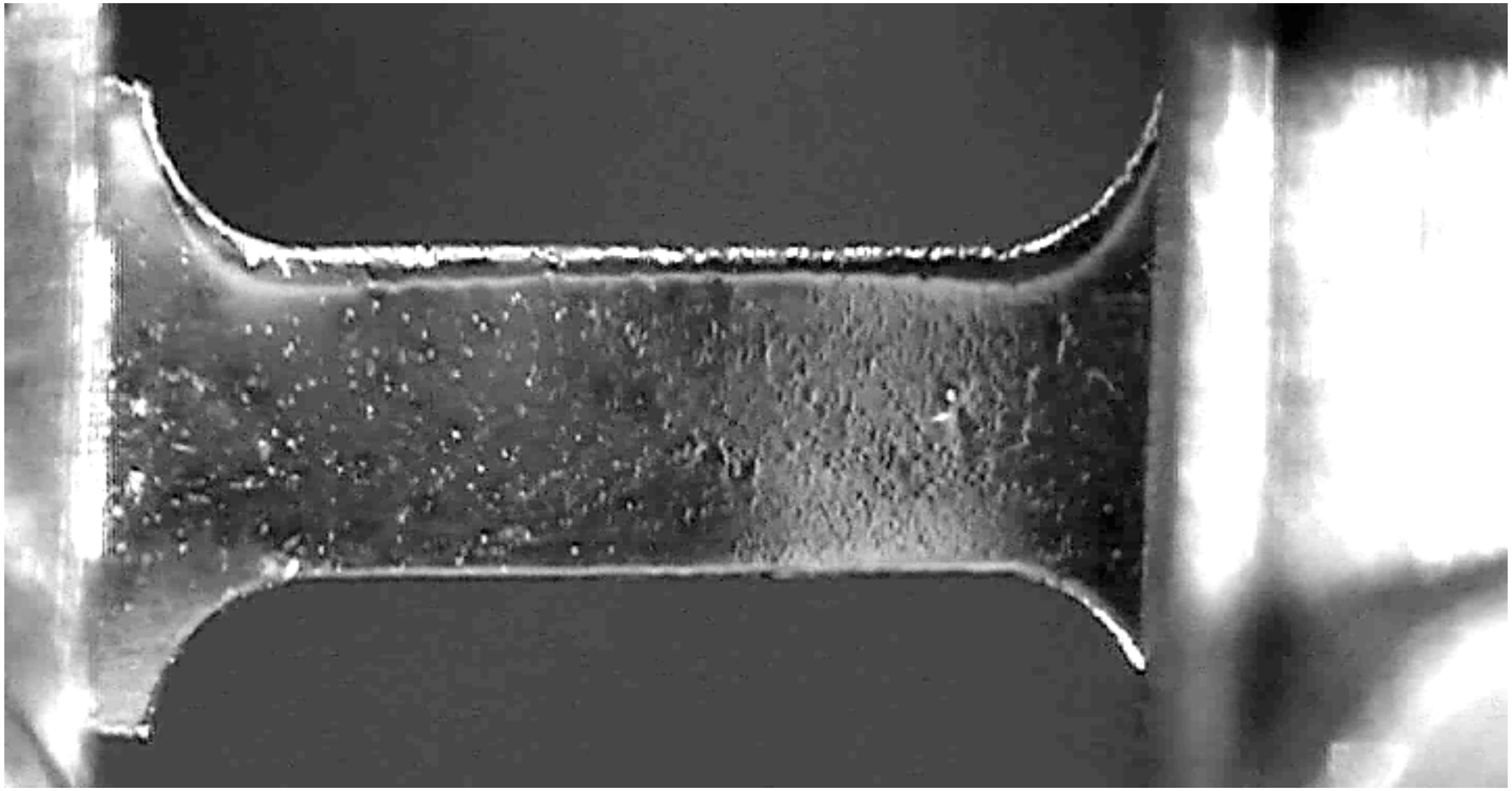

Single crystal pure Ni, unirradiated
Deformed in uniaxial tension at 5×10^{-5} s^{-1}
Traction axis: <110>
Test duration: 3.5 hours, elongation: ~120 %

Introduction

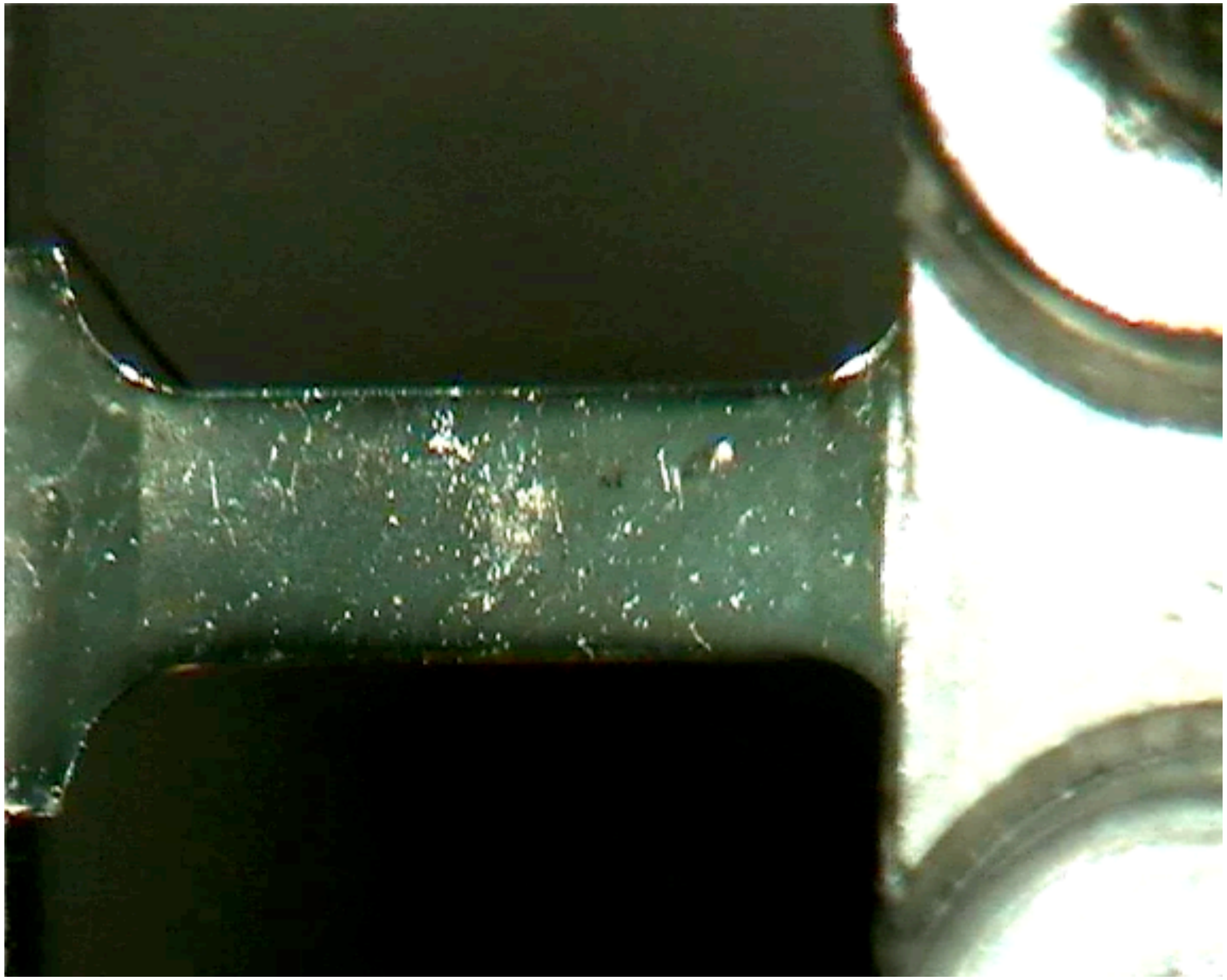

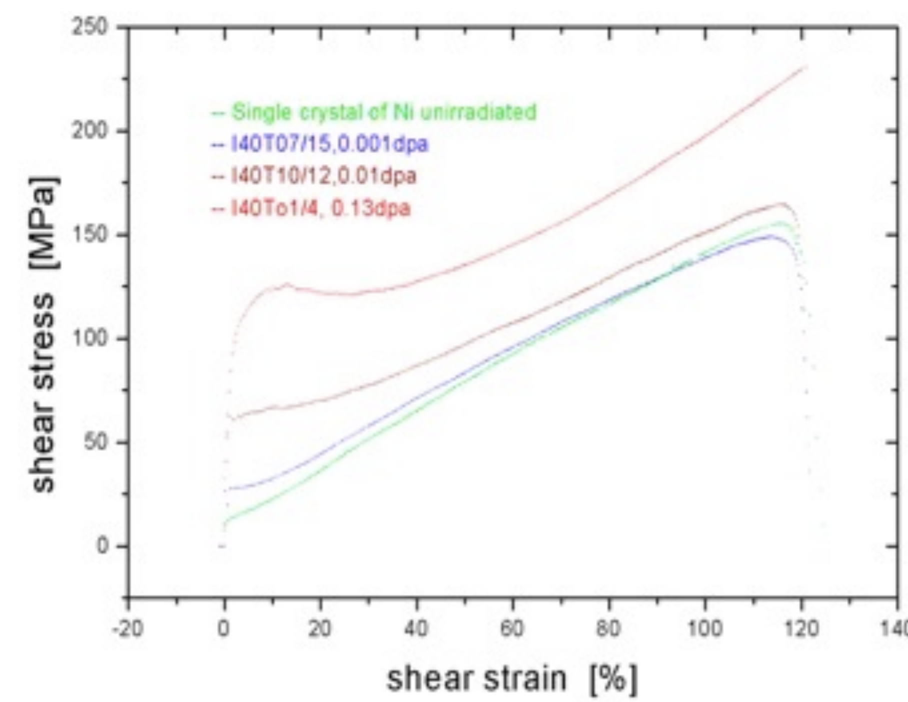

Single crystal pure Ni, irradiated to 0.1 dpa at RT
Deformed in uniaxial tension at $1x10^{-4}$ s^{-1}
Traction axis: <110>
Test duration: 2 hours, elongation: ~120 %

- Strong impact of radiation

Introduction

Ability to predict radiation induced effects ?

e.g. hardening, due to interaction of the defects with dislocations, vector of plasticity:

$$\Delta\sigma = \alpha \, \mu \, b \, [Nd]^{1/2}$$

Need for accuracy in the determination of:
- Defect density (N)
- Defect size (d)
- Defect type (α)

While **TEM** remains the only technique to directly observe these defects but it suffers from two limitations:

1) The size of the radiation induced damage and of the dislocation-defect interaction is at the limit of the TEM resolution (about 1 nm).
2) The time of reactions of defects is generally below the time resolution of the TEM (about 1/10 s).

> Need for proper characterization and modelling of radiation induced damage we have to take advantage of recent advances in TEM

Transmission electron microscopy: a brief history

1924: De Broglie associates the notion of wave length to particles
1927: Davisson, Gerner and Thomson demonstrate electron diffraction
1931: Ruska and Knoll obtain images with the first TEM
1933: The resolution of light microscopy is overcome by TEM
1936: Scherzer demonstrates that the main lens aberrations cannot be eliminated
1938: Von Ardenne builts the first scanning electron microscope
1939: First commercial electron microscopes are delivered
1941: The first EELS measurement recorded in TEM, by Ruthemann
1951: First microanalyzer of X-ray by Castaing
1965: Crewe describes the first STEM built at ANL
First quantification of the TEM image formation using the contrast transfer function by Hanszen and colleagues
1968: First experiments on off-axis holography
1980: Decisive progress made on electron tomography
1986: Nobel prize to Ruska, Binnig and Rohrer for the TEM
1994: First commercial image energy filter in TEM
1998: Cs corrector installed on a TEM by Haider et al, 1.3 Å
1999: Cs corrector installed on a STEM by Krivanek
2003: first commercial TEM with Cs correction
2008: improvement in Cs correction, 'TEAM' project, 0.5 Å
2009: Cs + Cc correctors, 'TEAM' project
2010: 'Low voltage' Cs corrected TEM, 'SALVE' project

TEM spatial resolution

TEM resolution suffers from spherical and chromatic aberrations

Spherical aberration C_s :

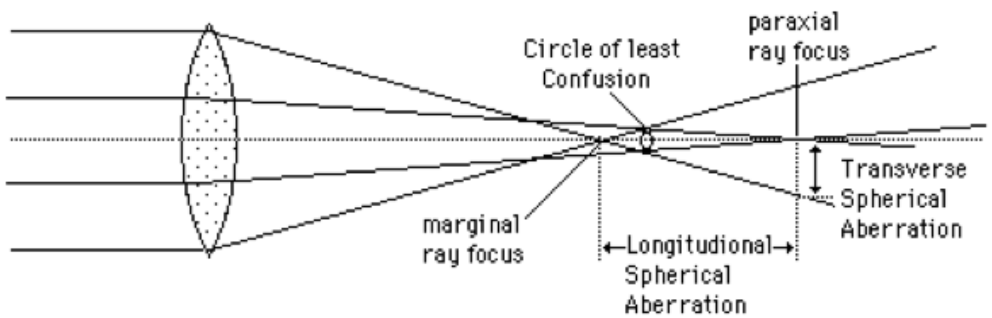

Resolution: $d = 0.6\,(C_3 \cdot \lambda)^{1/4}$

The advent of C_s correction end of the 90s, made possible thank to computing power, allowed a quantum leap in spatial resolution :

First Cs corrector in 1998 on a TEM resulted in a resolution of 1.3 Å, starting from a 'conventional' resolution of 2.4 Å.
Haider et al, Journal of Electron Microscopy, 48 (1998) 395-405

More recently, an ultimate resolution of just below 0.5 Å was reached, within the 'TEAM' US project that comprises 5 DOE labs. It is the 'TEAM 0.5' Cs corrected TEM at Berkeley NCEM, open to users in 2008.

'TEAM I' : C_s + C_c correction TEM at Berkeley NCEM, 2009

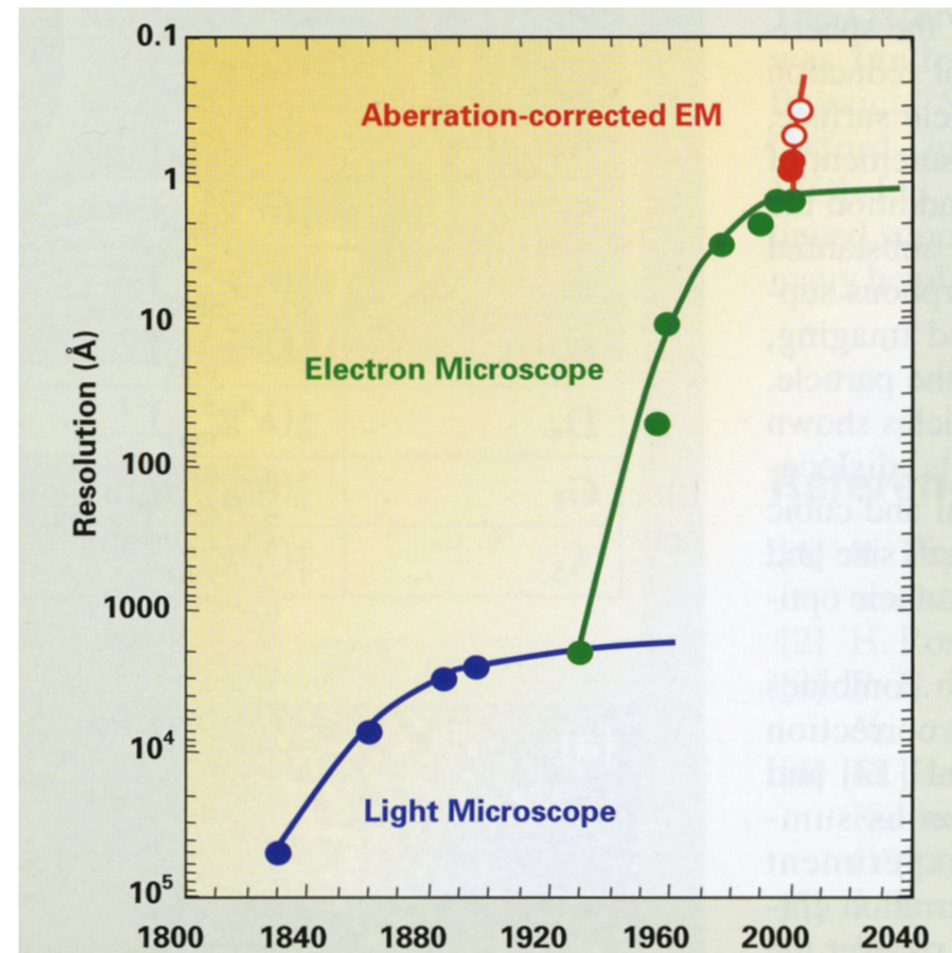

A.I. Kirkland et al., JEOL News 41 (1) (2006) 8-11

nice but the price tag of the 'TEAM 0.5' is 7 M€ ... to be compared to 500 k€ for a conventional TEM

The TEM wheel

Conventional TEM
TU Vienna

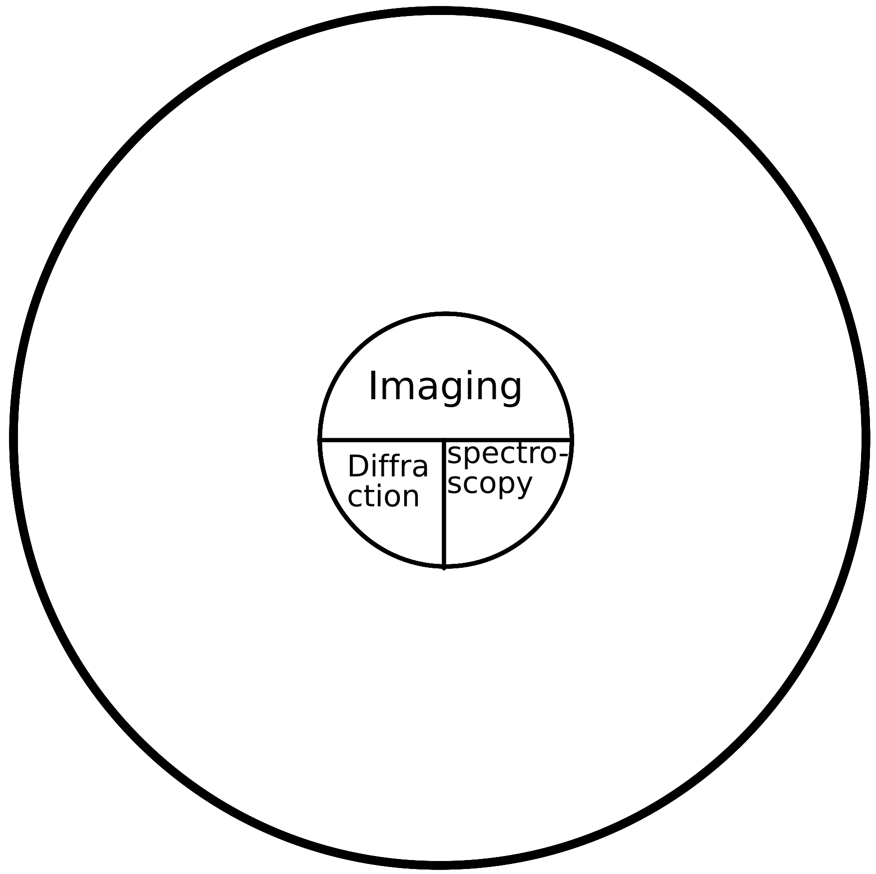

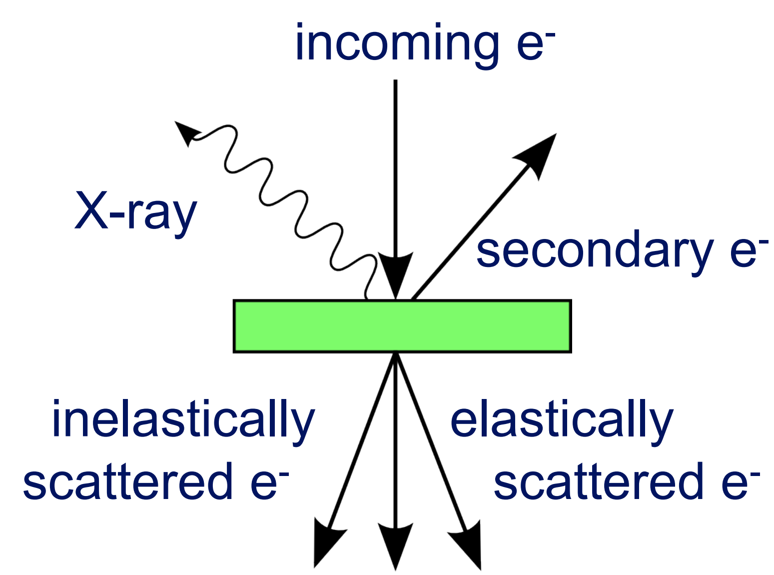

The TEM wheel

Cs corrected STEM

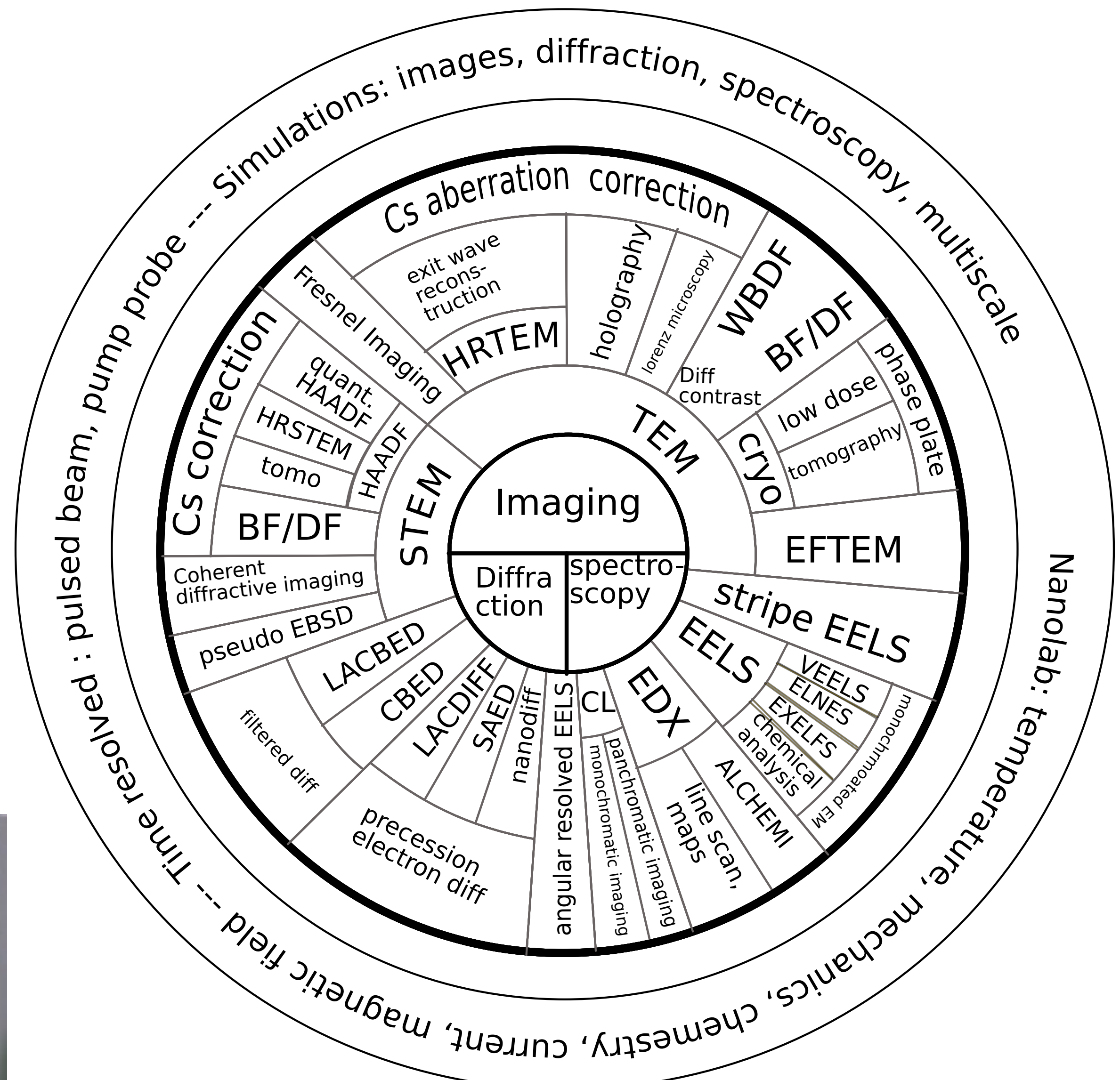

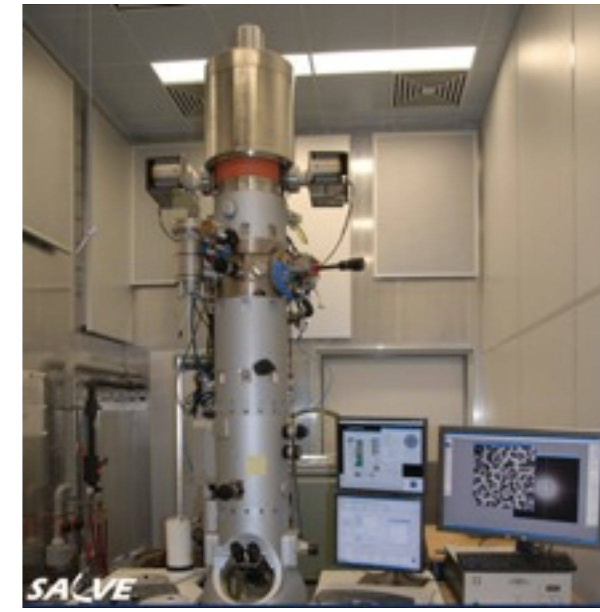

Low voltage Cs corrected TEM Ulm

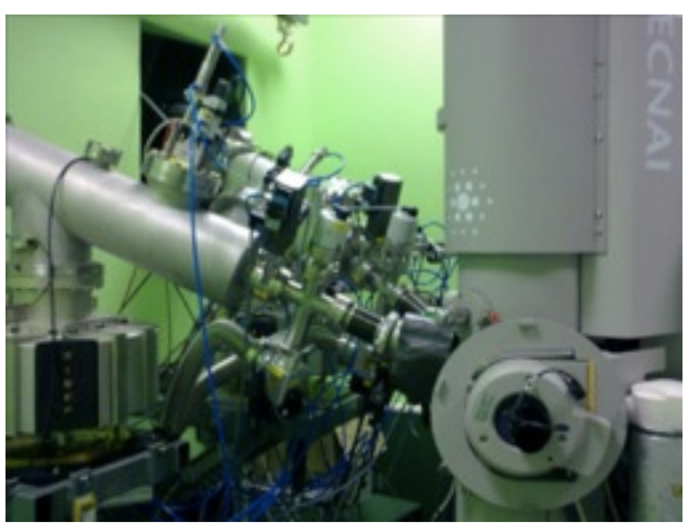

TEM in situ dual implantation JANNuS Orsay

EFTEM

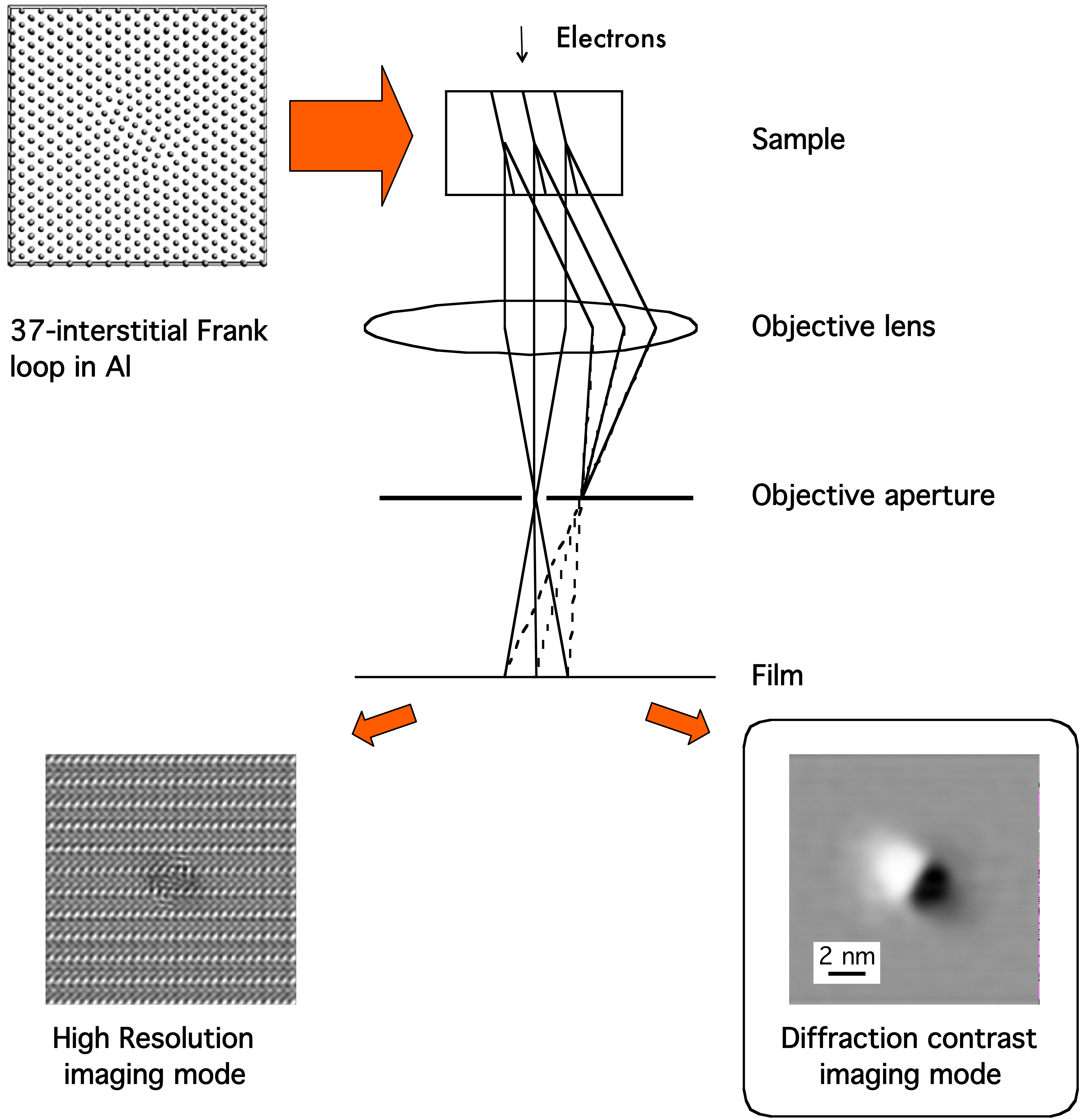
Electrons
Sample
Objective lens
Objective aperture
Film
37-interstitial Frank loop in Al
High Resolution imaging mode
2 nm
Diffraction contrast imaging mode

TEM imaging using diffraction contrast

Crystal defect

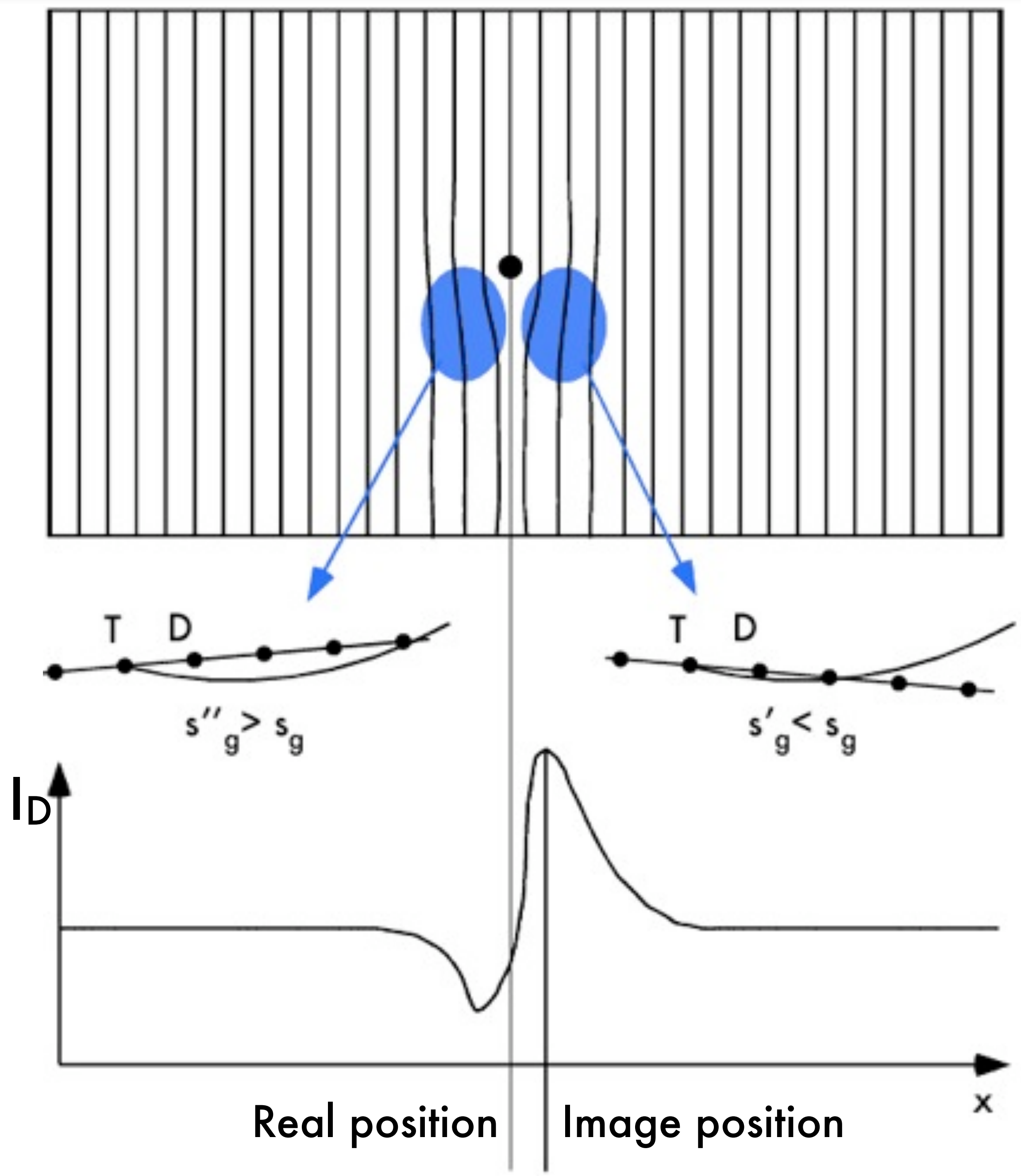

Diffraction condition in the perfect crystal:

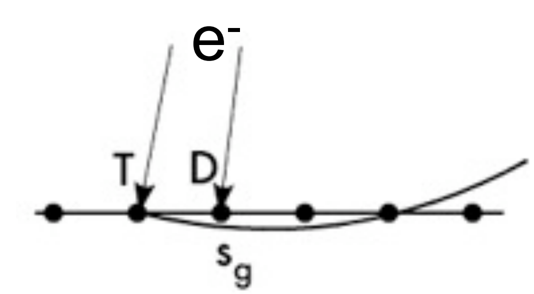

Width of contrast: 1/3 extinction distance

$$\xi_g^{eff} = \frac{\xi_g}{\sqrt{1 + s_g^2 \xi_g^2}}$$

Position of the maximum intensity close to the 'turning point': $\mathbf{g}.\partial \mathbf{R}/\partial z + s_g = 0$

D. J. H. Cockayne, I. L. F. Ray and M. J. Whelan, Phil. Mag. 20 1265 (1969)

- 'Weak beam': dark field with weakly excited imaging beam

CONVERGENT WEAK BEAM TECHNIQUE

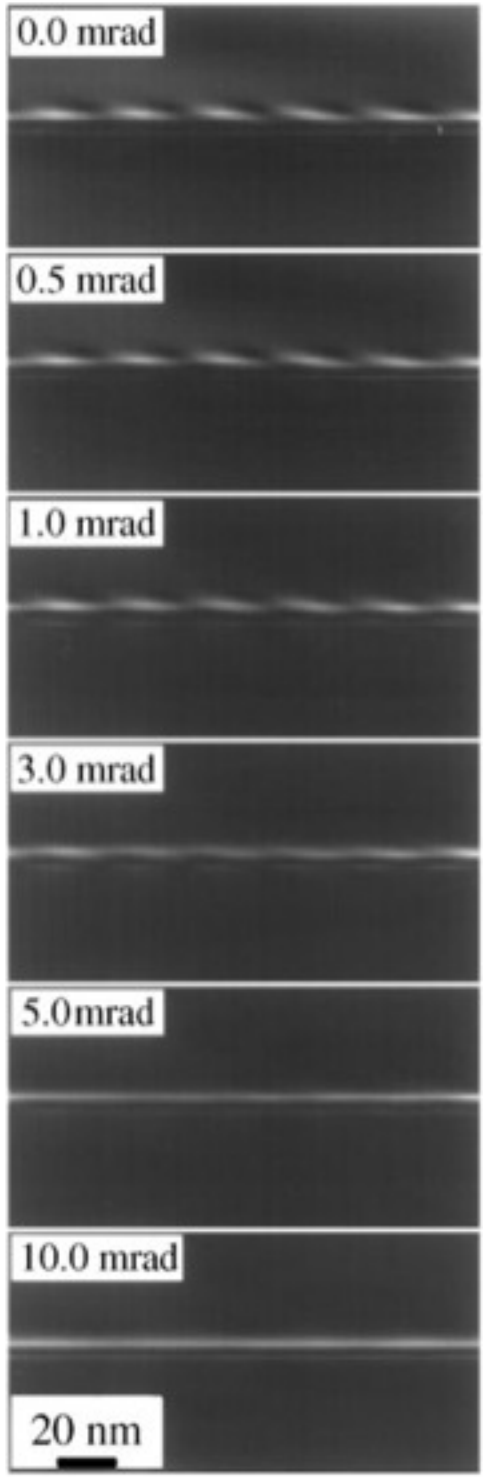

Simulated WB-TEM g(3.1g) image of an edge dislocation in Cu with convergence angle

thickness oscillations → DEFECTS ARE INVISIBLE at some depths!

Script for TEM JEOL2010: tilting the incident beam allows to achieve a range of conditions around the selected diffraction condition in a single exposure of the photographic negative

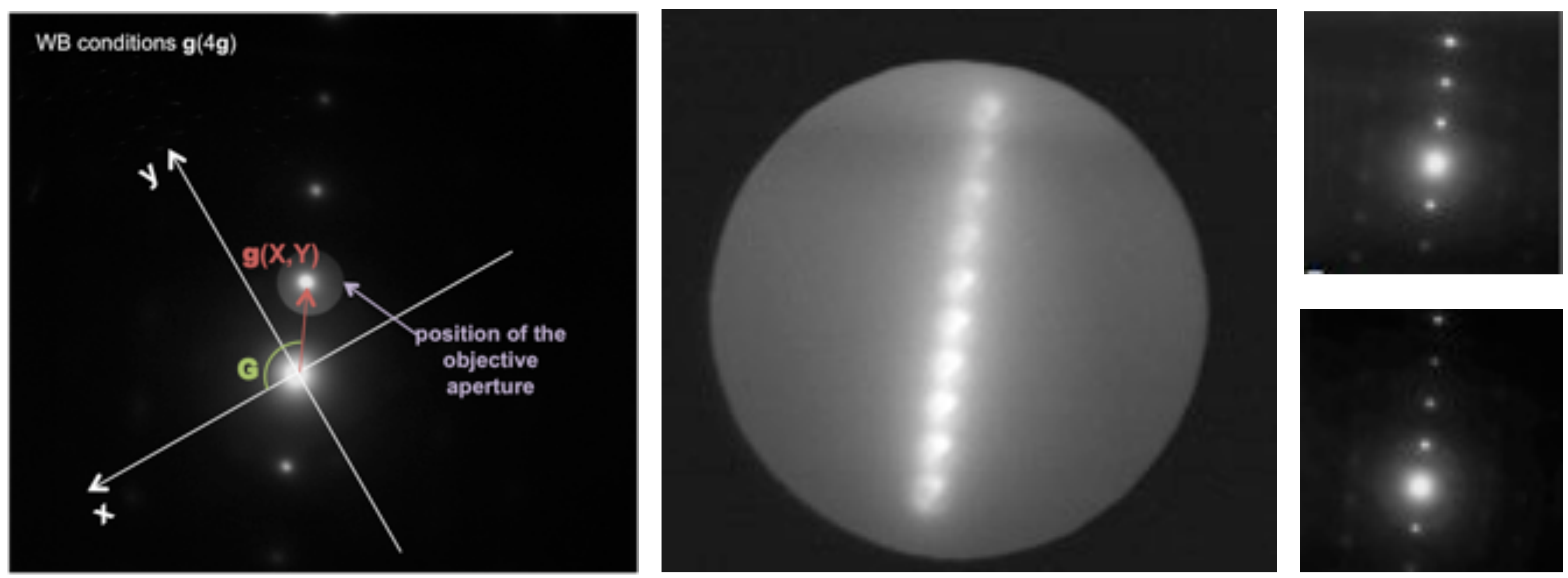

A. Prokhodtseva CRPP

R. **Schäublin** et al. Ultramicroscopy 83 (2000)

CONVERGENT WEAK BEAM TECHNIQUE

UHP Fe CRPP irradiated at RT with 500 keV Fe ions in situ at JANNuS Orsay

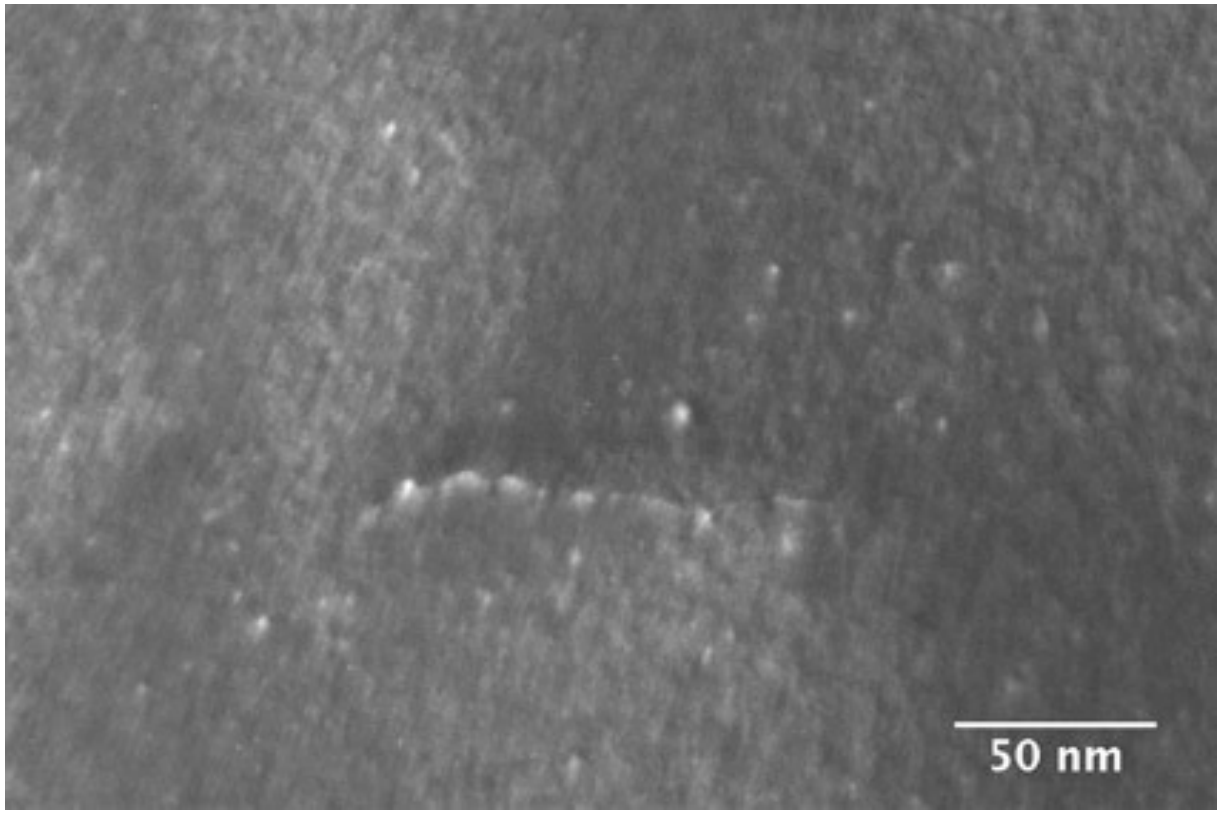

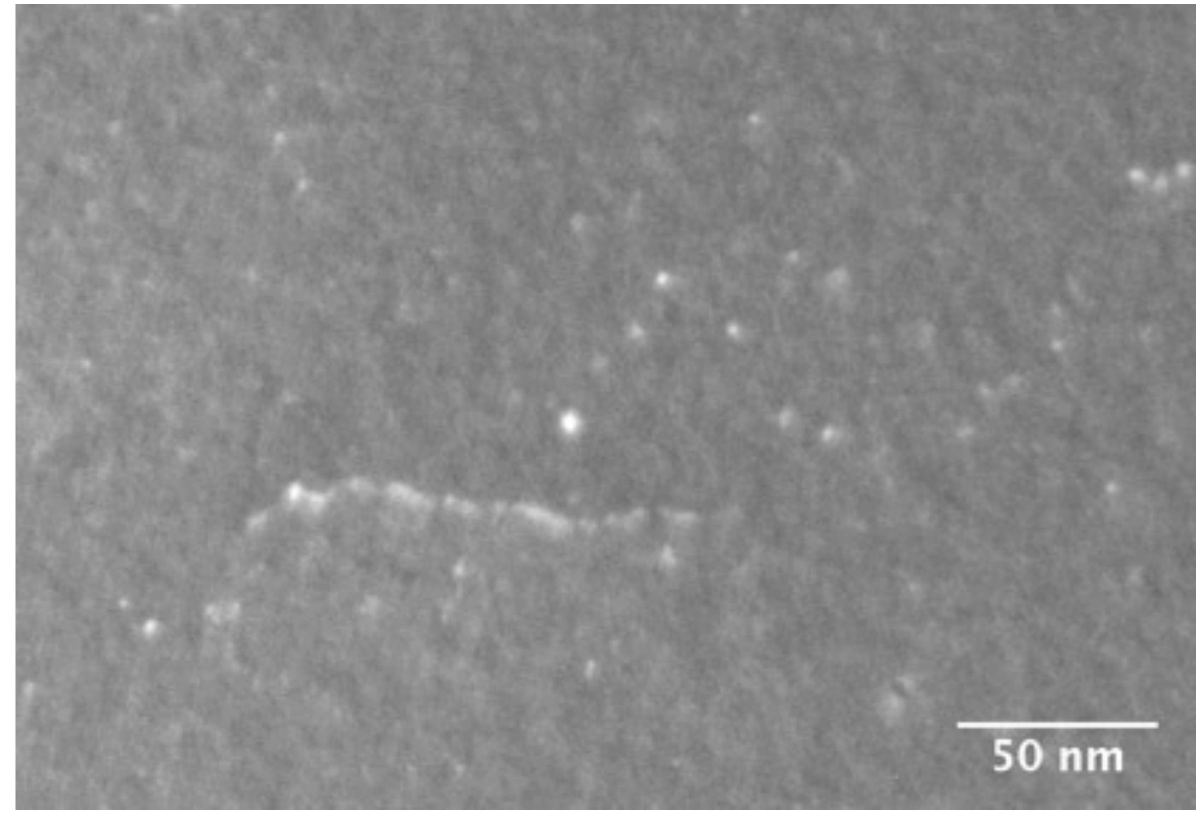

WB **g**(4**g**) image
Beam is centered within the objective aperture

Thickness: **~150 nm**
Defect number density: **$1.2 \cdot 10^{22}$ m^{-3}**

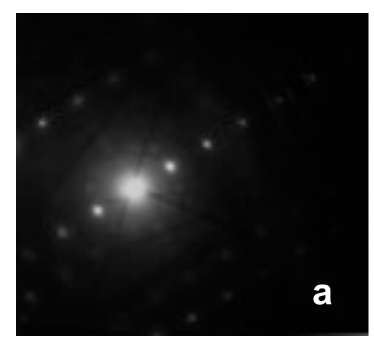

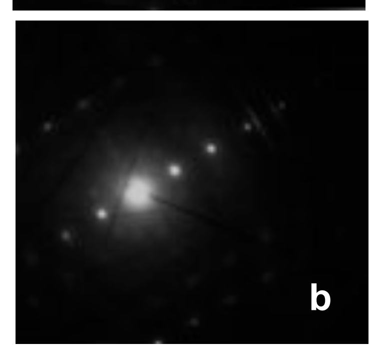

CWB image taken in 11 sec single exposure with the range of conditions from (a) to (b)

Thickness: **~150 nm**
Defect number density: **$1.5 \cdot 10^{22}$ m^{-3}**

CWBT will be used for more efficient g·b analyses of irradiated samples

~25% more defects are detected

TEM imaging using diffraction contrast

Limiting factors in the imaging of small structures:

The objective aperture ?

- Necessary to obtain diffraction contrast,
- But it cuts out higher spatial frequencies.
- Typical objective aperture (for bright field, dark field and weak beam dark field imaging modes) limits the resolution of the microscope to about 6 to 7 Å.

- A new aperture was designed by image simulation, on an MD simulated defect.
- Rectangular in shape, placed perpendicular to the operating diffraction vector g (to avoid taking other g's). It implies that resolution is improved along the long axis of the aperture.

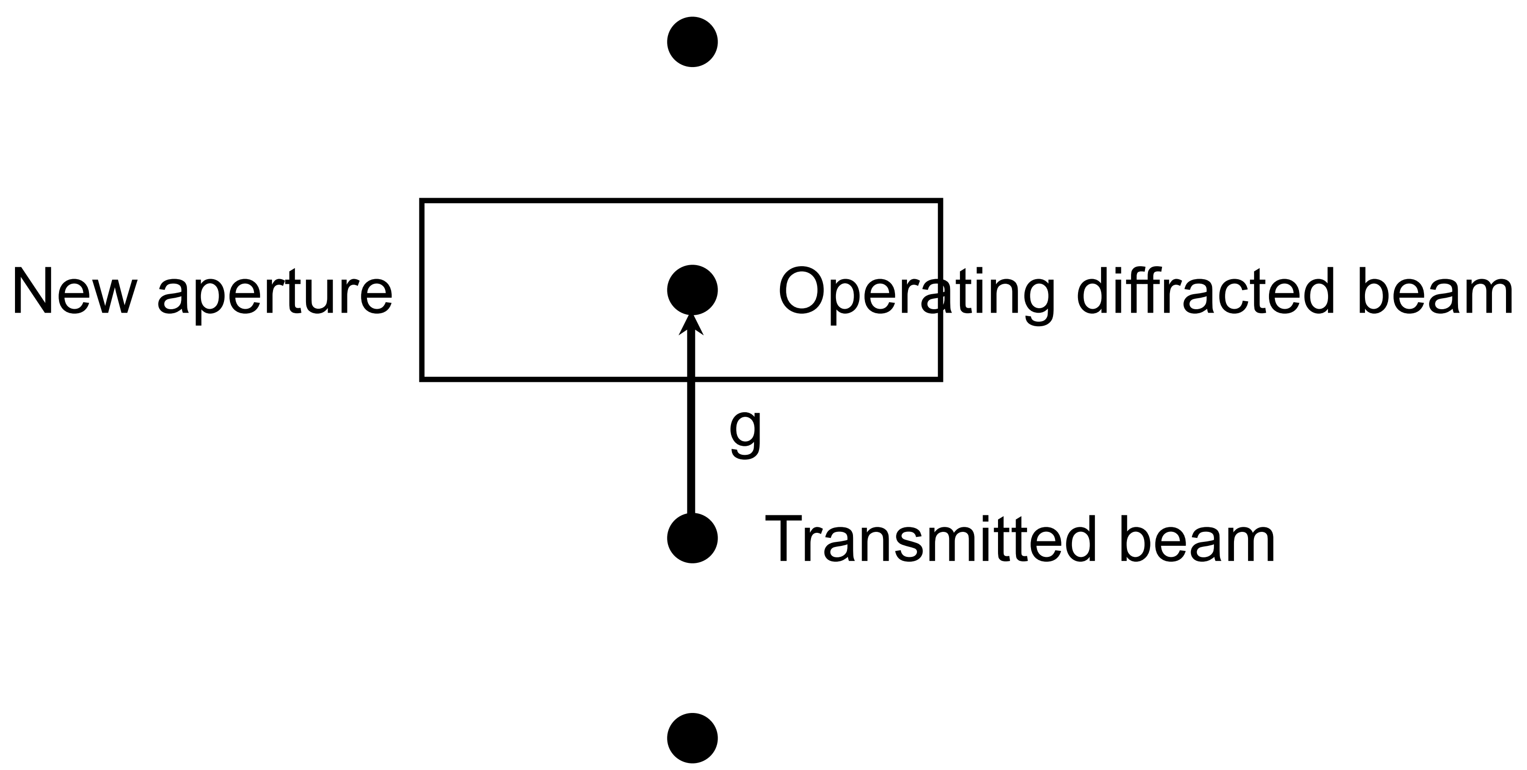

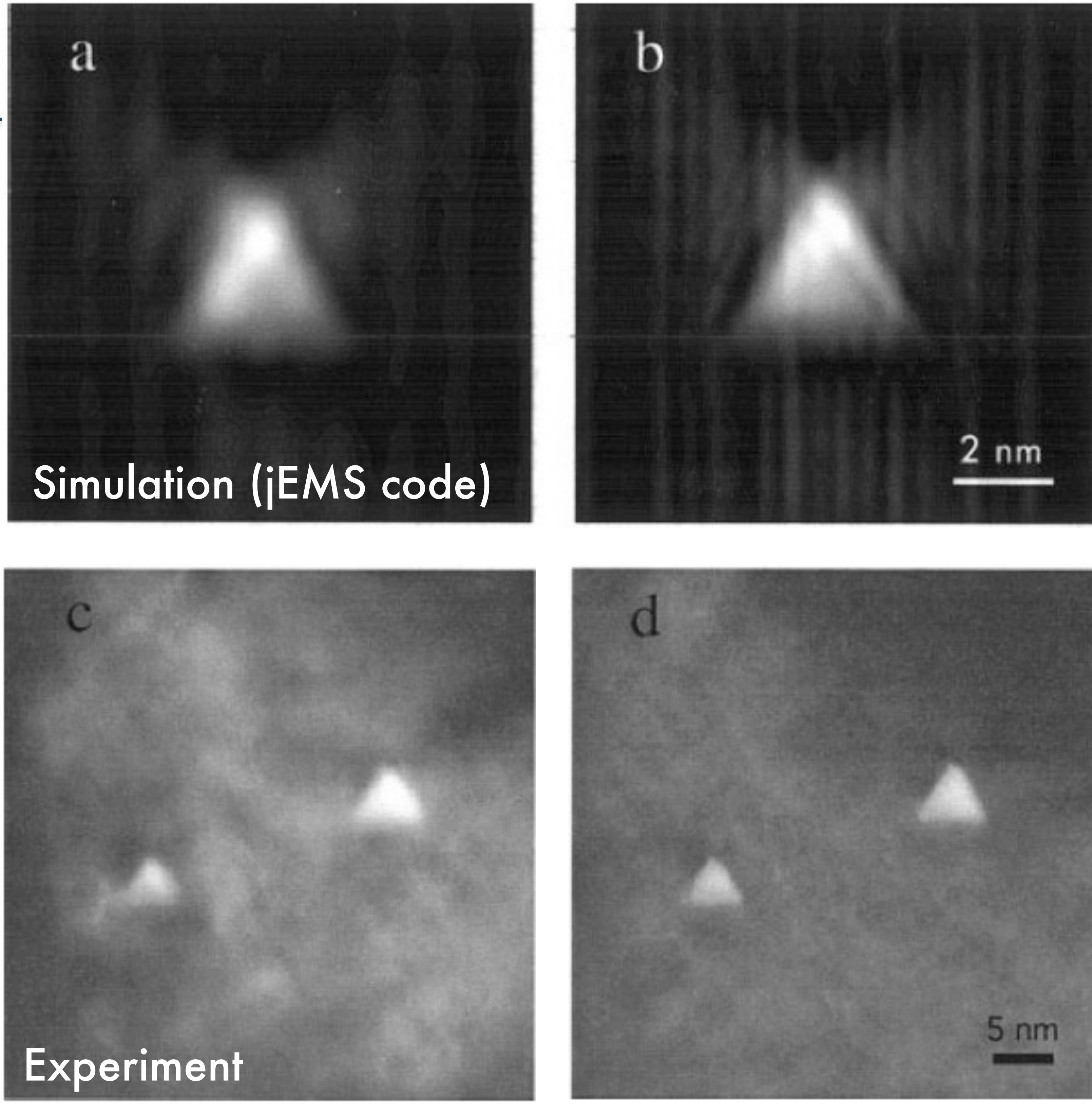

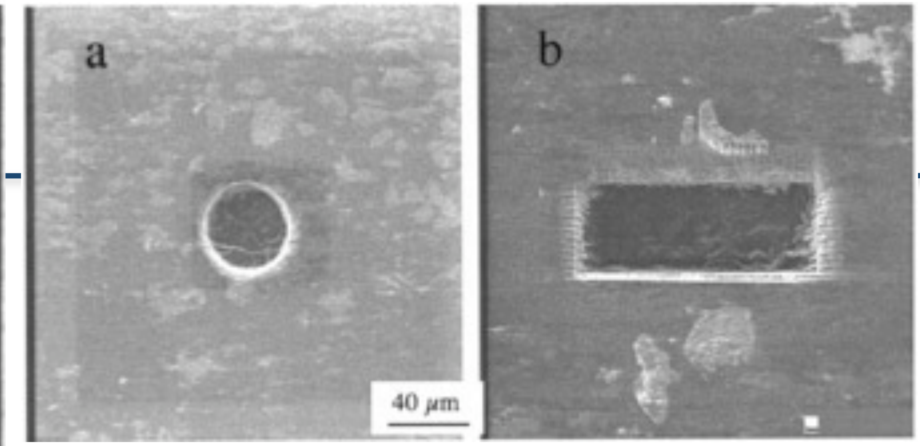

Fig. 14. SEM micrograph of the apertures cut by FIB in a 15 μm thick Mo foil with a size of (**a**) ϕ 40 μm and (b) 40 × 100 μm^2.

Collab. with N. Nita, Sendai Univ.

New objective aperture design:

Improved resolution in diffraction contrast:
from 6 Å to 3 Å

Fig. 15. Simulated (**a** and **b**) and experimental (**c** and **d**) weak beam TEM images, 200 kV, **g**(6g), {**g**200}, close to a zone axis <011>, of SFT, obtained with an objective aperture size of (a) 2.8 nm^{-1}, (b) 2.8 × 6.5 nm^{-2}, (c) ϕ 40 μm, and (d) 40 × 100 μm^2. Experimental images made in Au quenched in water from the melting temperature.

R. Schaeublin, Microscopy Research and Technique 69 (2006) 305-316

- Drastic improvement in spatial resolution

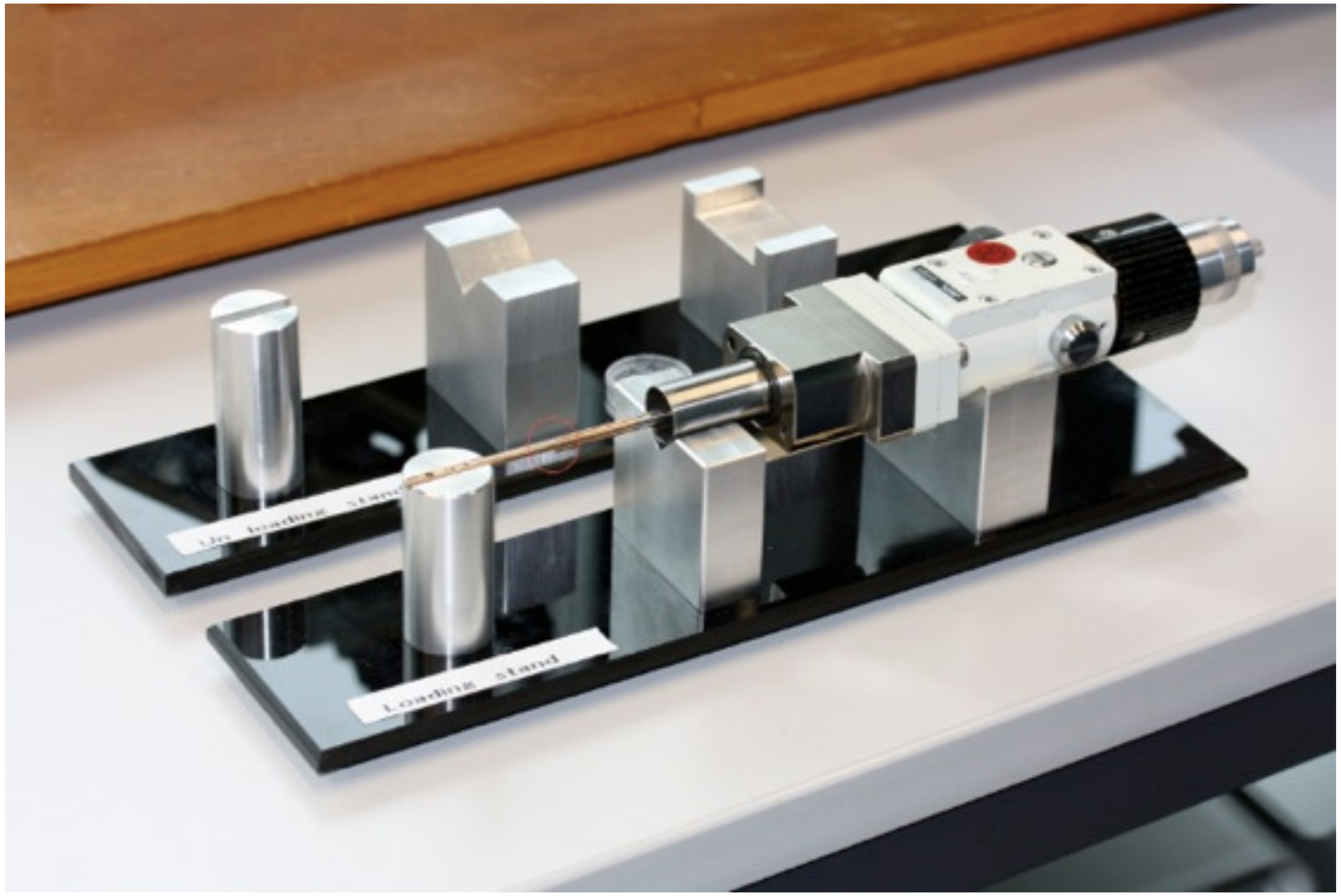

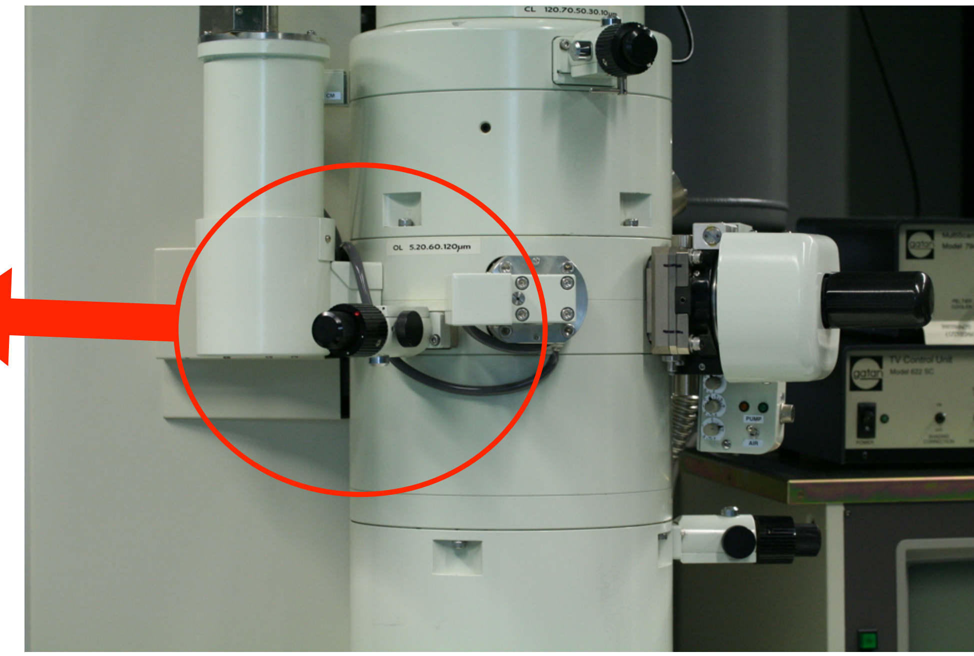

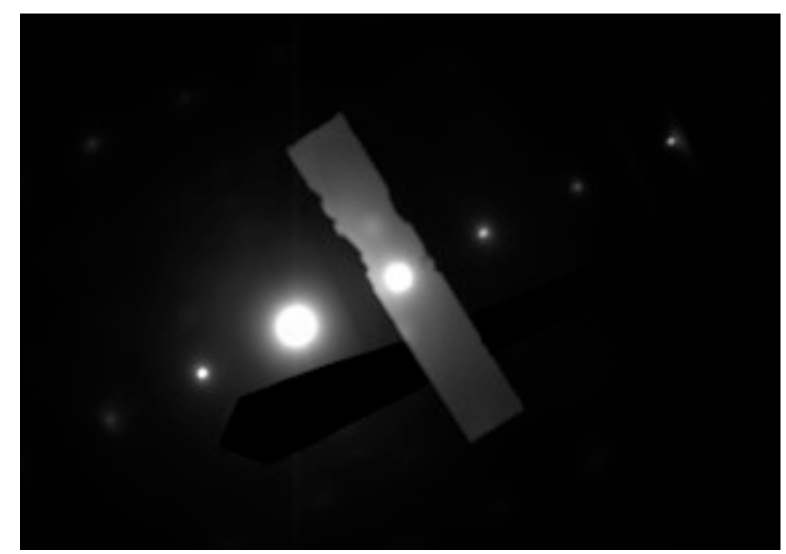

Modified objective aperture holder of TEM JEOL 2010: Design of a new aperture rotation mechanism allowing orienting the aperture perpendicular to the operating **g** .

- Manufactured by EMS® (Bolton, UK), delivered 2011
- Its 3 apertures are cut by FIB

(ø 10, ø 20 µm and 20x120 µm^2)

TEM imaging of microstructures

How can we further improve on imaging of complex structures ?

TEM BF

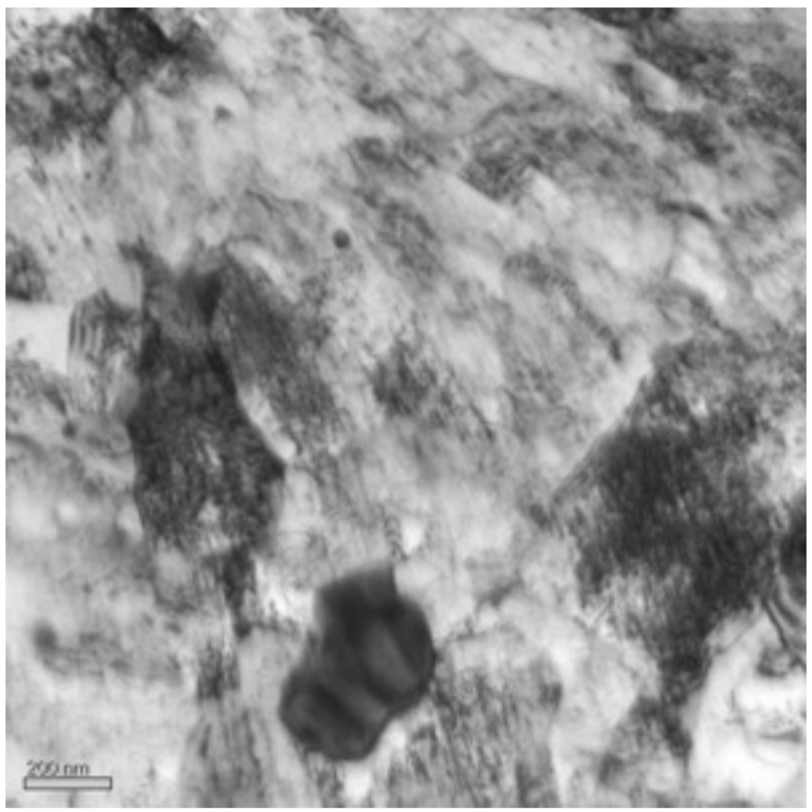

EFTEM BF elastic

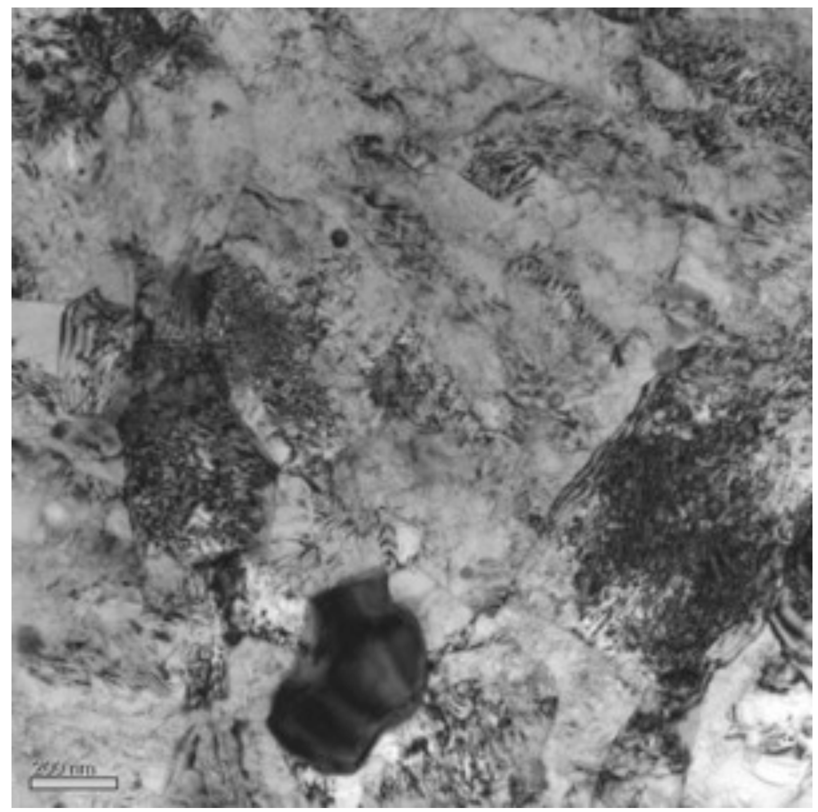

STEM UHAADF

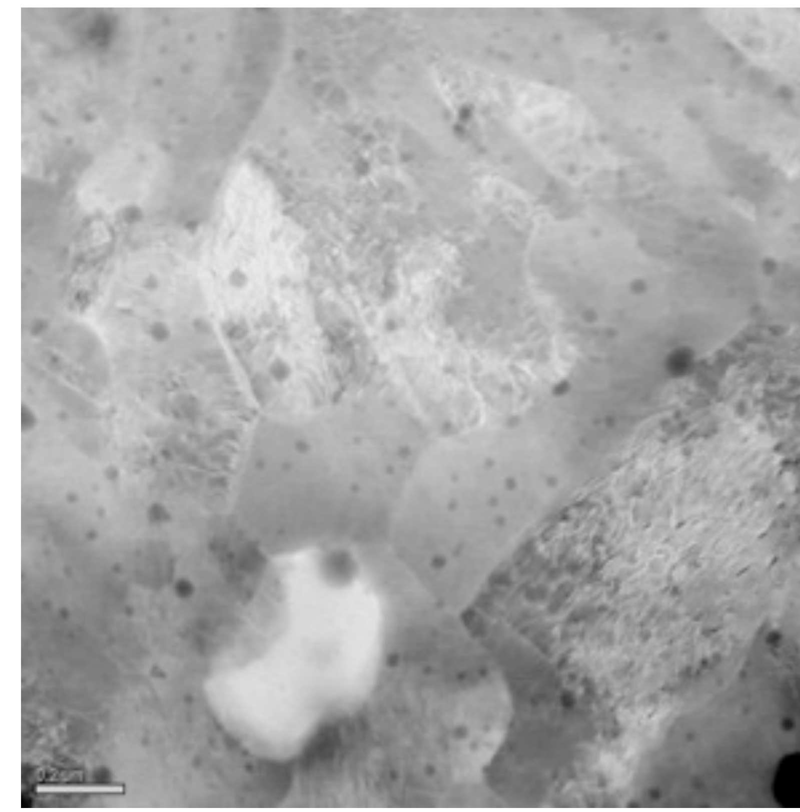

Model ODS ferritic steel: 83.4Fe, 14Cr, 2W, 0.3Ti with $0.3Y_2O_3$ nanoparticles, CRPP EPFL
TEM, EFTEM, STEM: JEOL 2200FS @ CIME EPFL Lausanne

- Zero loss energy filtering (elastic imaging) reduces noise, especially in thick regions
- High angle dark field STEM improves imaging: highlights oxides, grain structure

TEM imaging of microstructures

TEM BF

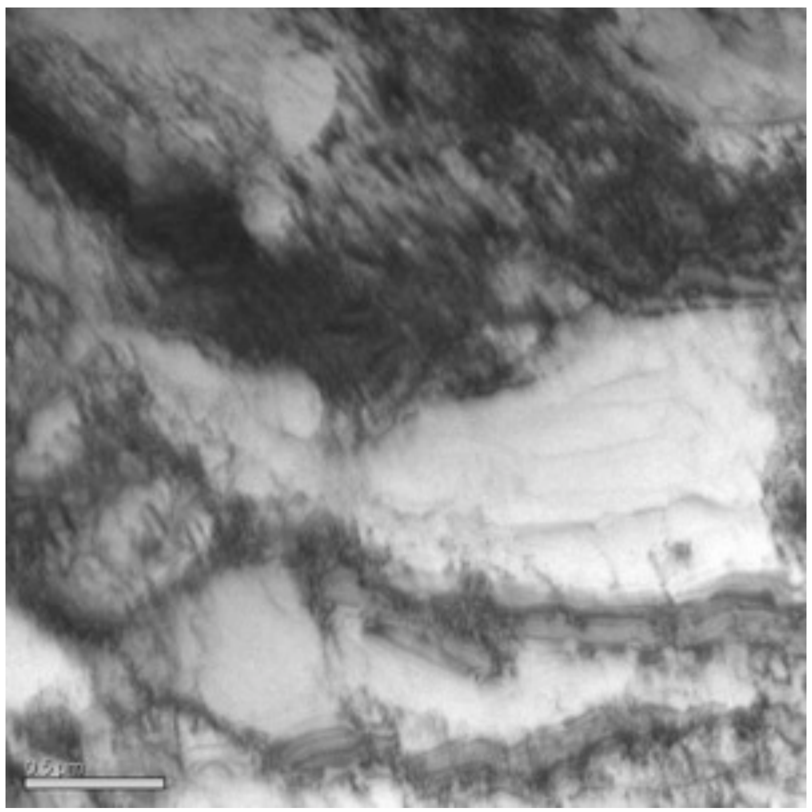

EFTEM BF elastic

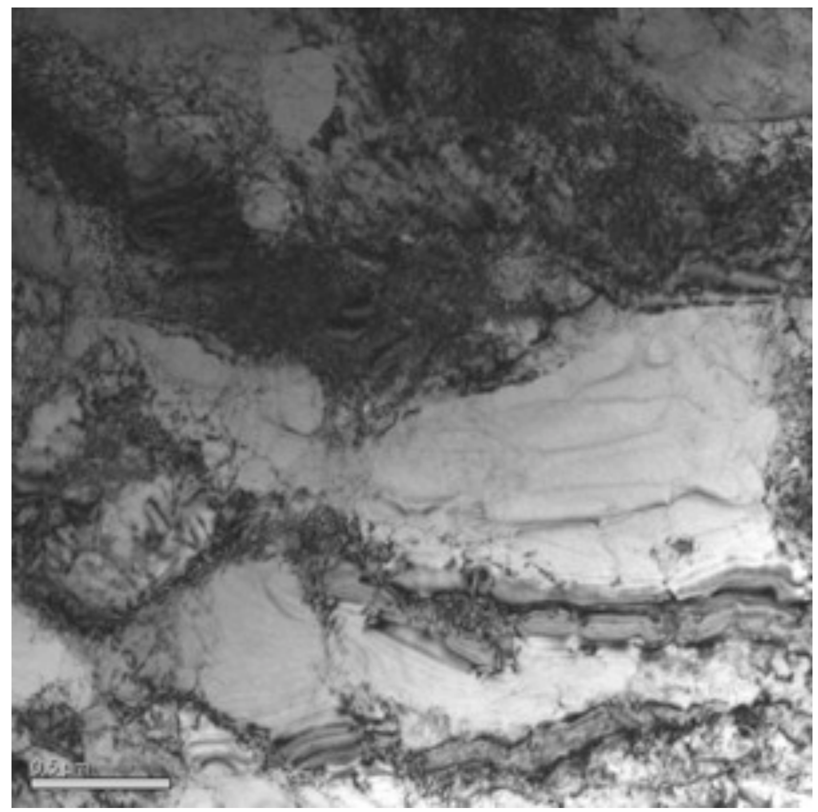

STEM UHAADF

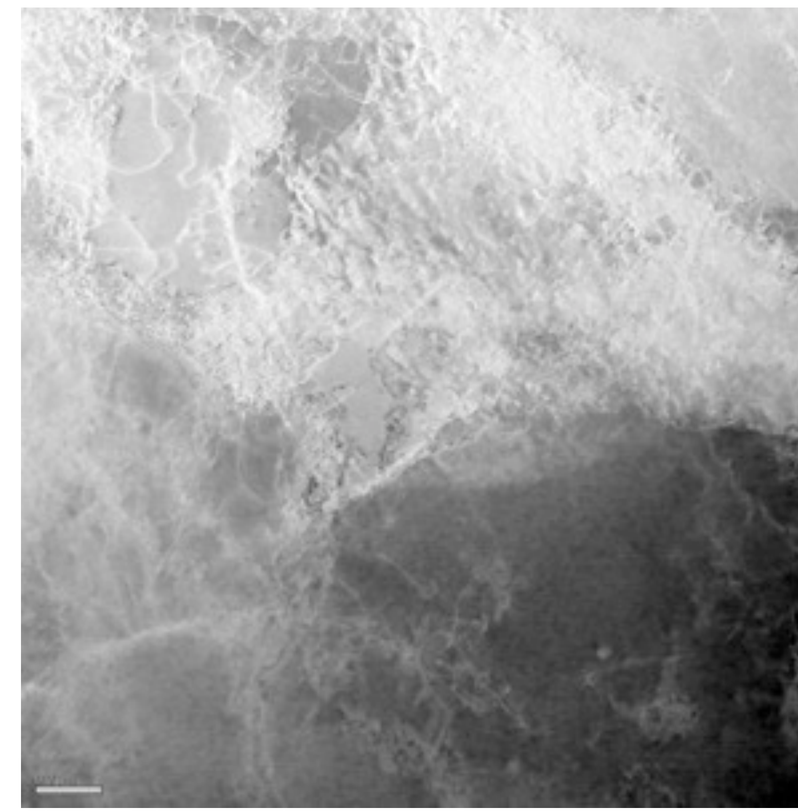

Model ferritic steel: UHP Fe-5Cr, EFDA, for Mössbauer study, S. Dubiel, Cracow
TEM, EFTEM, STEM: JEOL 2200FS @ CIME EPFL Lausanne

- Zero loss energy filtering (elastic imaging) reduces noise, especially in thick regions
- High angle dark field STEM improves imaging: highlights grain structure in deformations

Comparing STEM and TEM

STEM BF

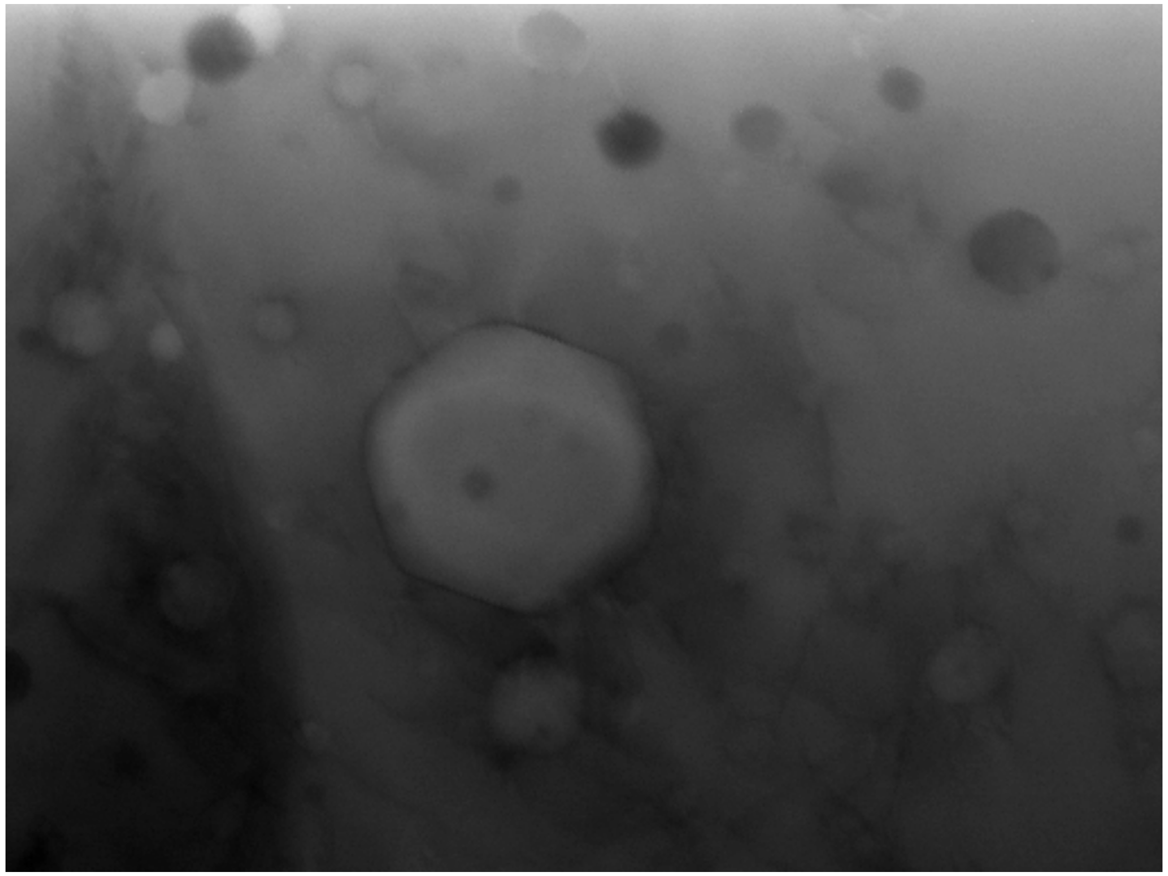

TEM

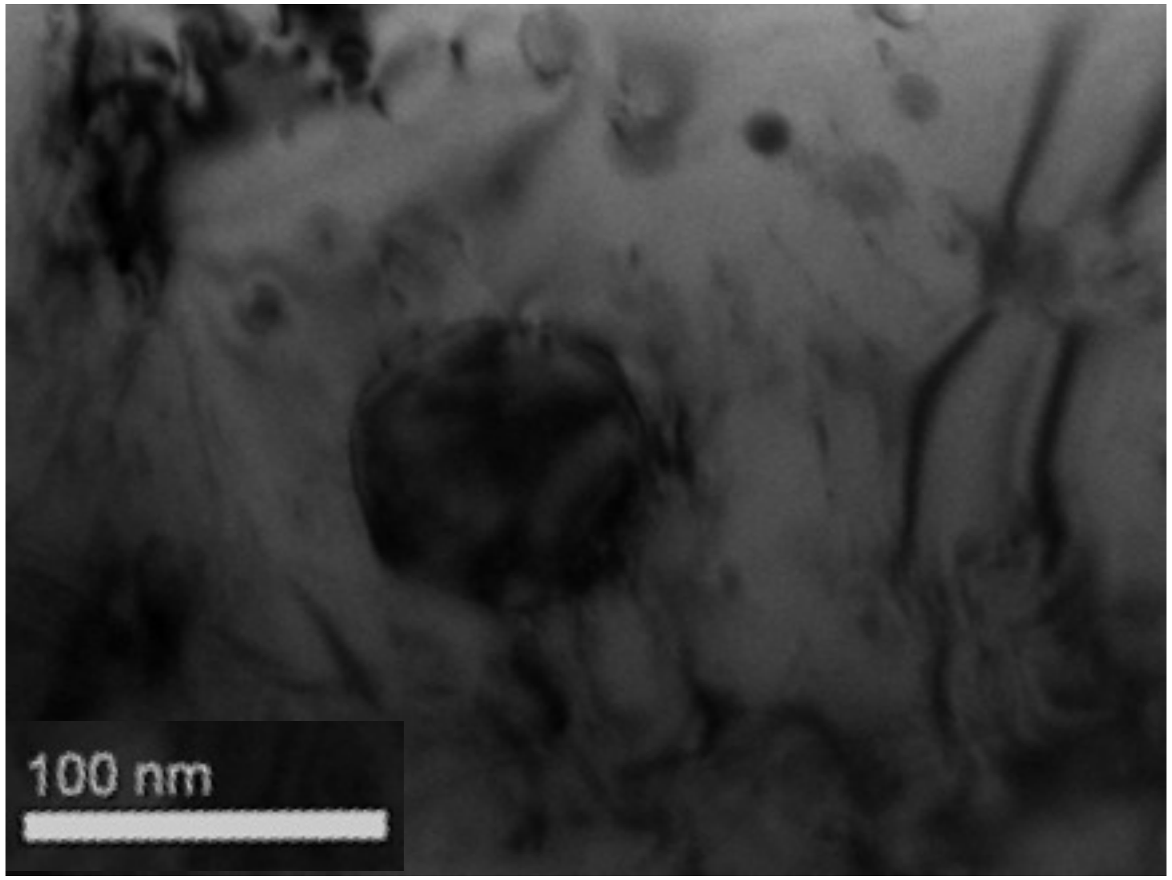

STEM: Hitachi HD2700 Cs corrected, 0.8 Å
T. Plocinski WUT
TEM: JEOL 2200FS, C. Hébert CIME EPFL

Model ODS ferritic steel: 83.4Fe, 14Cr, 2W 0.3Ti, 0.3Y_2O_3, CRPP EPFL

EFTEM thickness map: t/λ, λ = ~110 nm
→ region of interest is ~150 nm thick

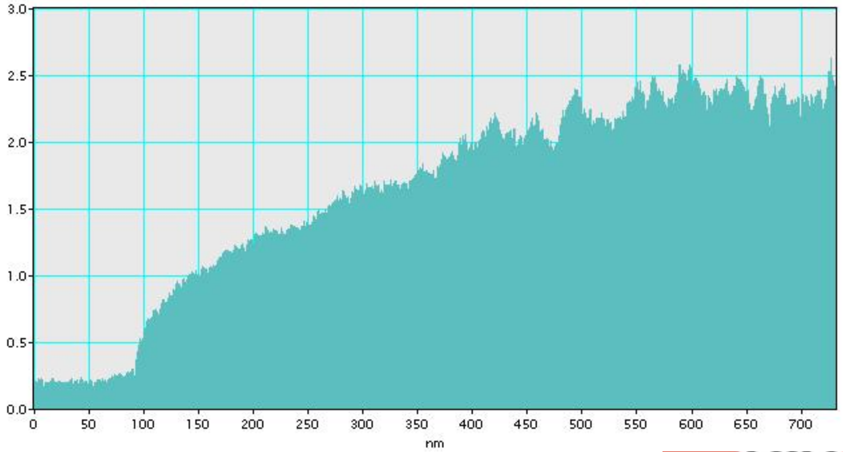

Comparing STEM X-ray EDS to EFTEM: chemical analysis

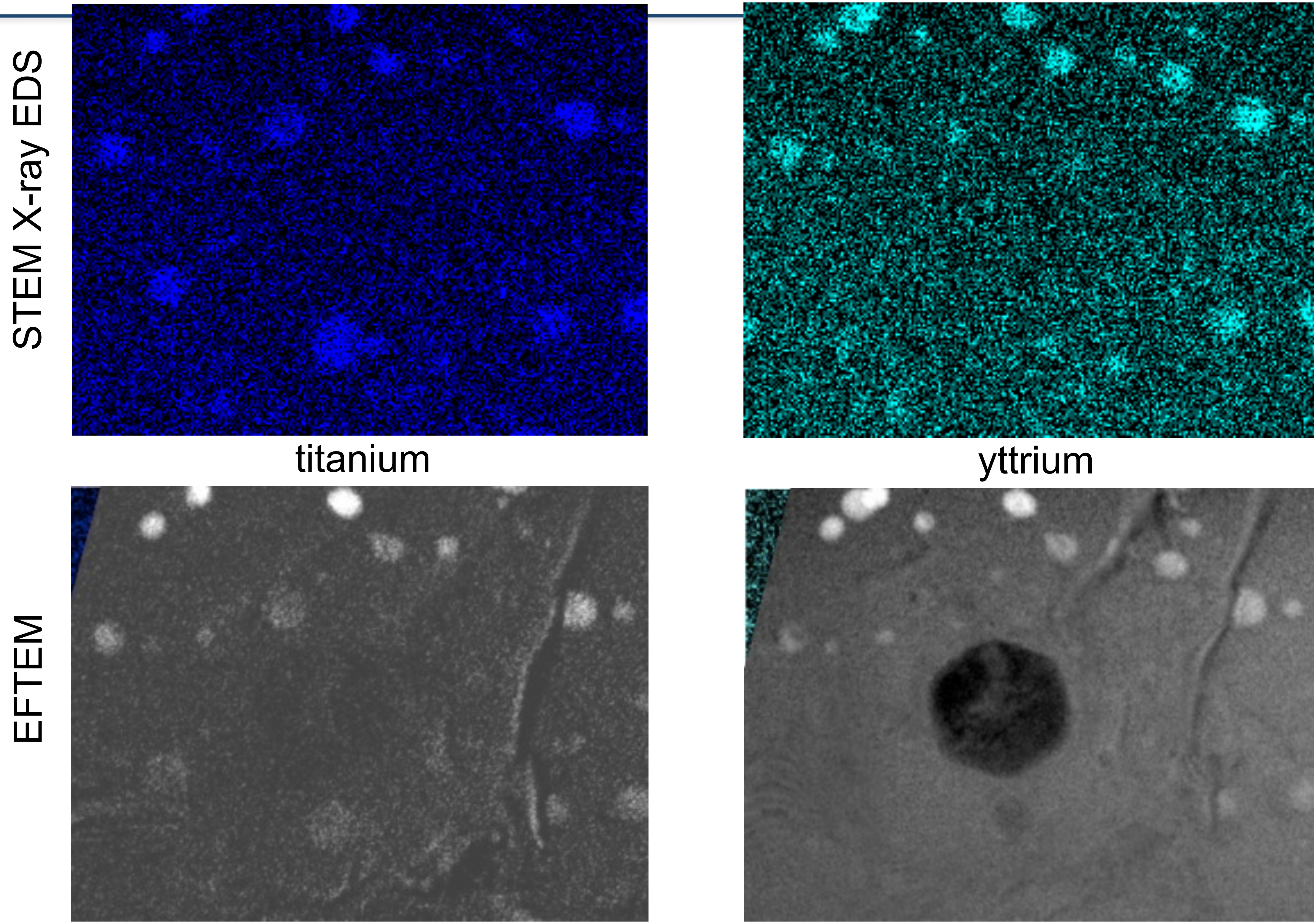

- Y : yttria (Y_2O_3)   Ti and Y : pyrochlore phase ($Y_2Ti_2O_7$ or Y_2TiO_5)
- **EFTEM more sensitive to sample thickness**

Comparing STEM X-ray EDS to EFTEM: chemical analysis

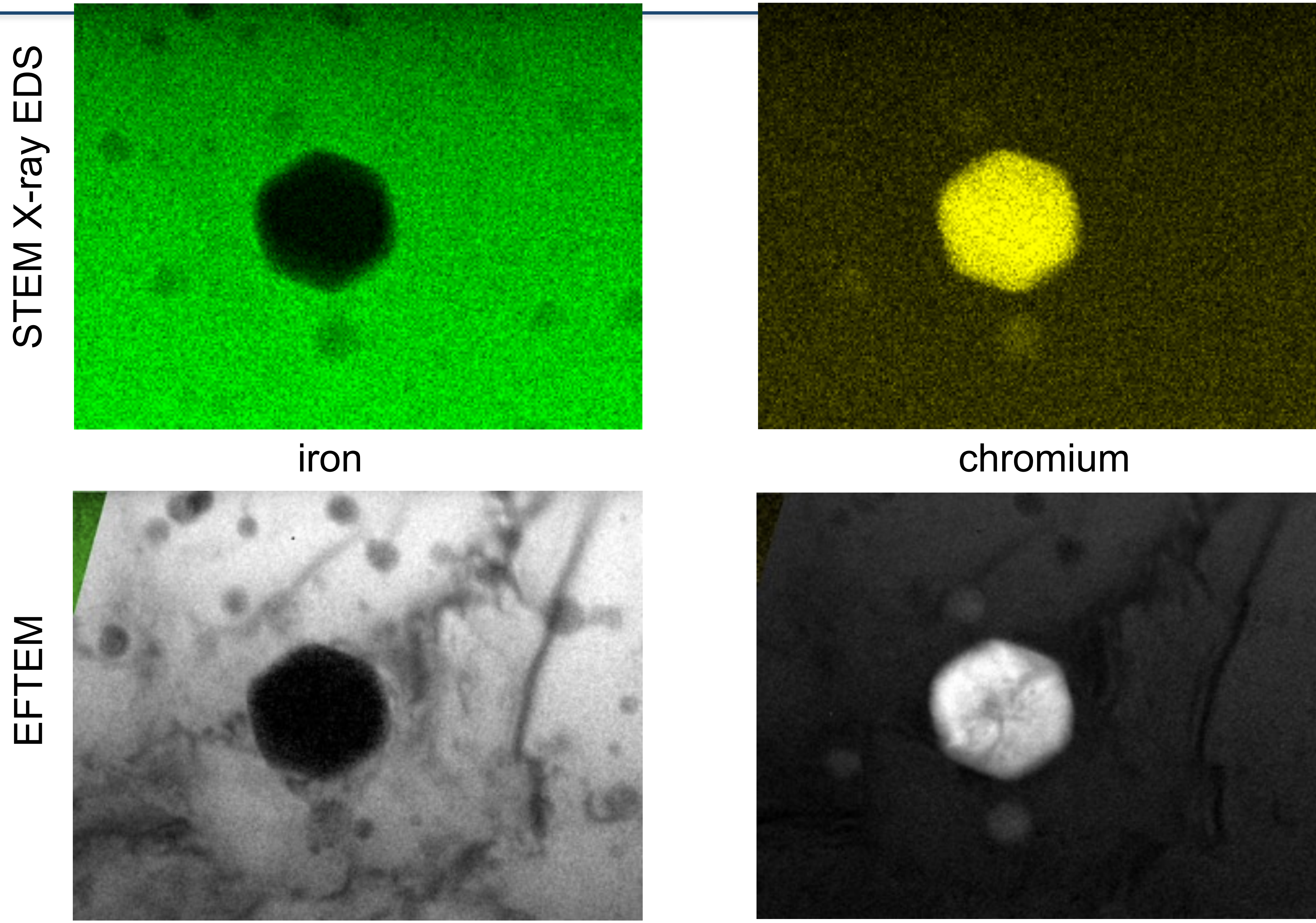

- **4 particles rich in Cr, in both STEM EDS and EFTEM**
- **EFTEM sensitive to diffraction contrast**

Comparing STEM X-ray EDS to EFTEM: chemical analysis

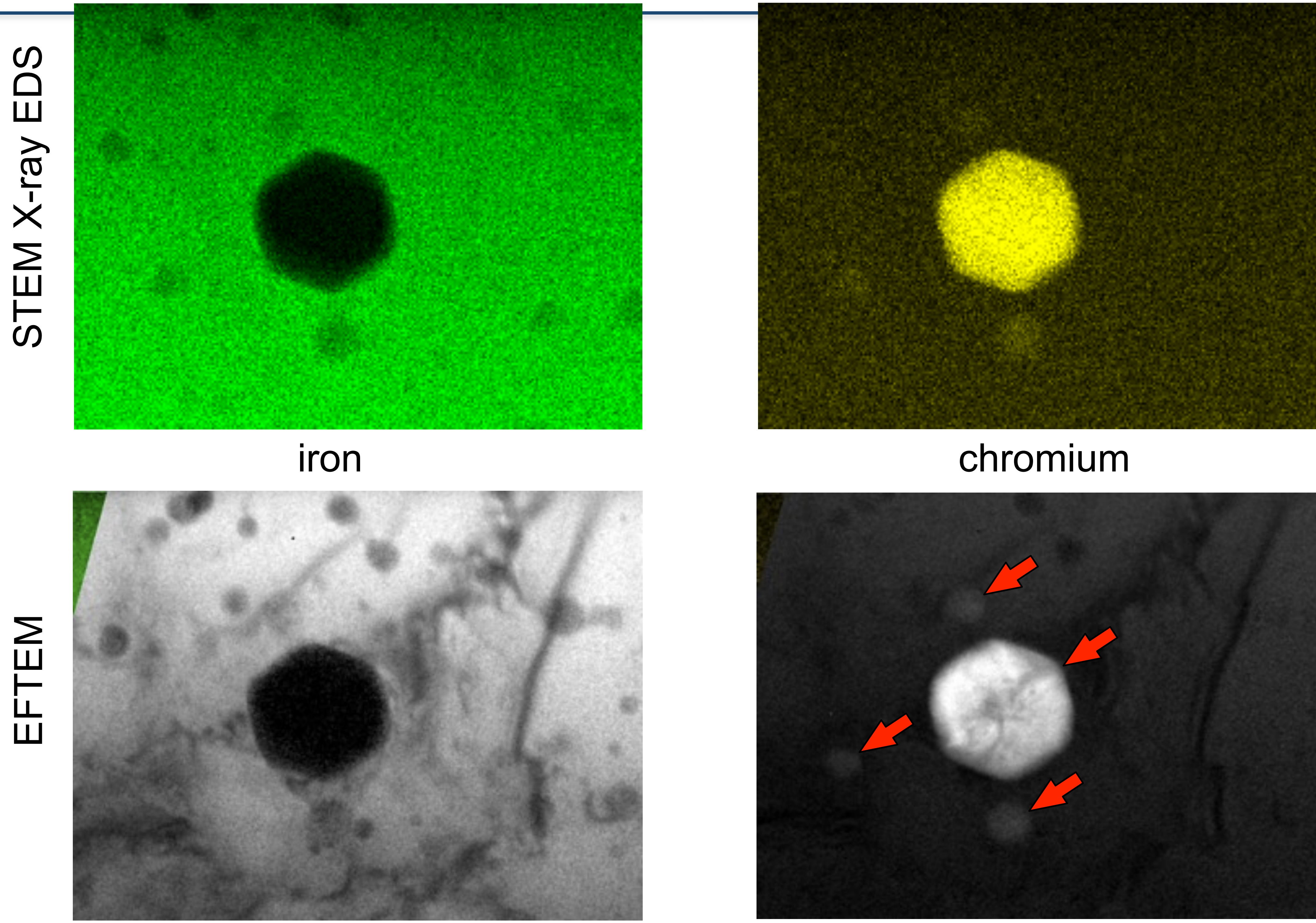

- **4 particles rich in Cr, in both STEM EDS and EFTEM**
- **EFTEM sensitive to diffraction contrast**

Comparing STEM X-ray EDS to EFTEM: chemical analysis

STEM X-ray EDS

oxygen ?

EFTEM

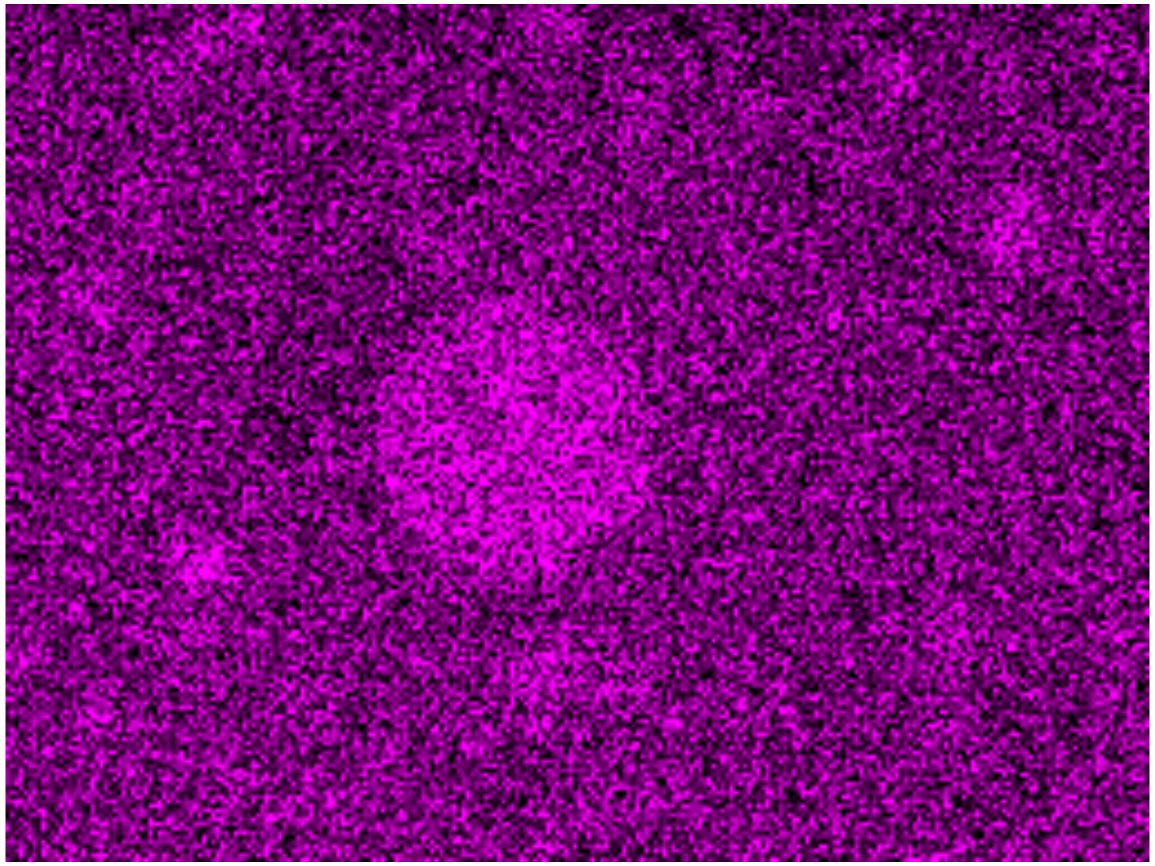

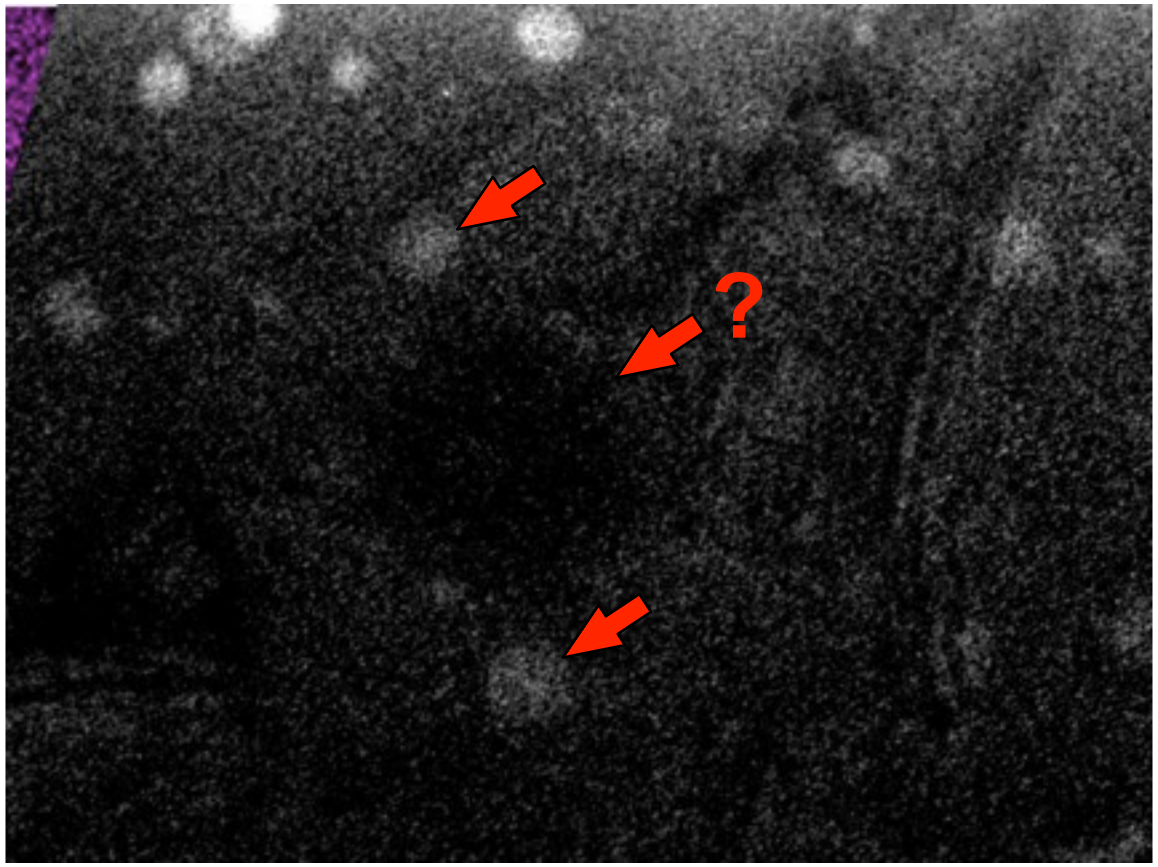

- **2 particles rich in Ti, Cr and O in both STEM EDS and EFTEM : Ti-Cr oxide**
- **large Cr rich particle : with or without oxygen ?**
- **EFTEM better for light elements than X-ray EDS :**

Comparing STEM X-ray EDS to EFTEM: chemical analysis

EFTEM : oxygen

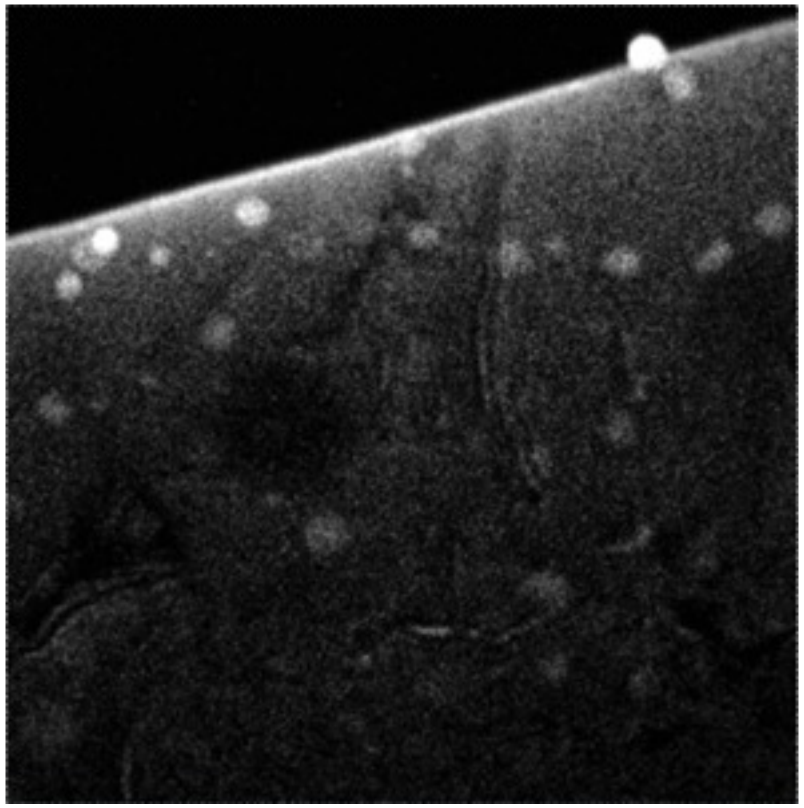

carbon

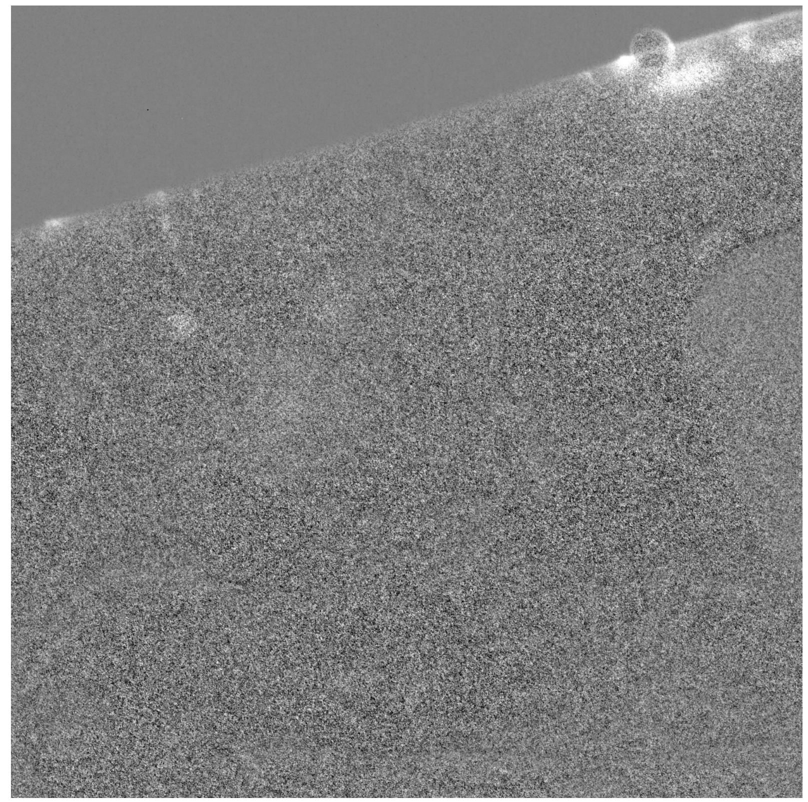

nitrogen

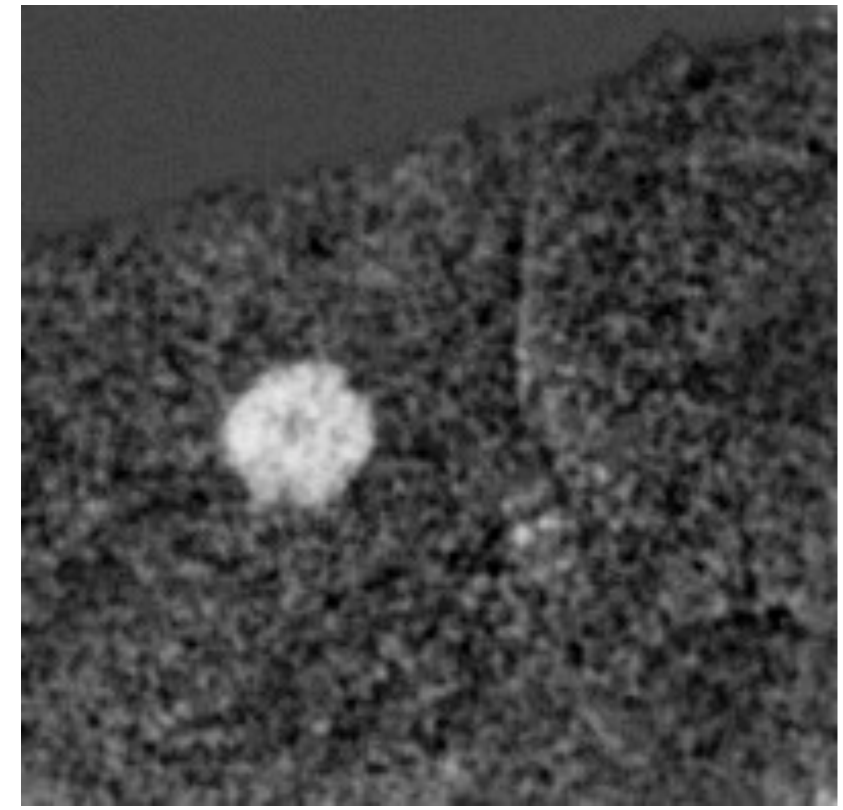

- **large particle is a Cr nitride**

Chemical analysis: comparing STEM X-ray EDS to EFTEM

Yttrium map

STEM X-ray EDS

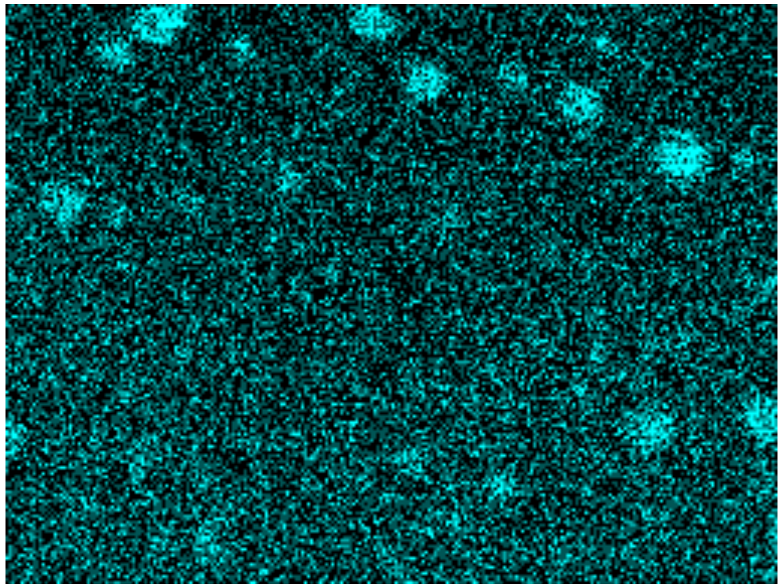

Image size: 431x324 pixels

EFTEM

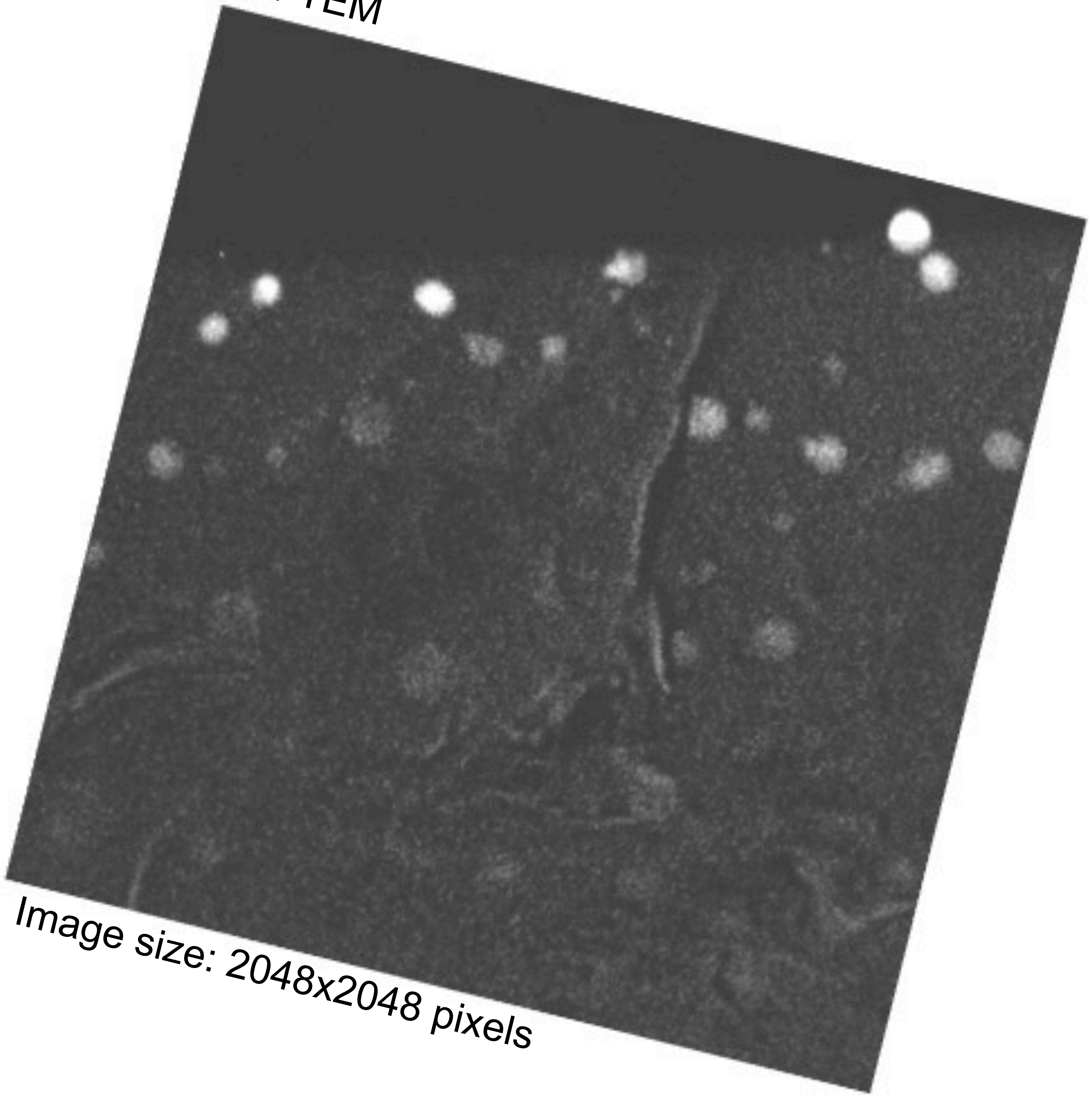

Image size: 2048x2048 pixels

- **Sampling: EFTEM does better than STEM EDS when considering acquisition time**
- **Spatial resolution: considering probe size for STEM, the number of electrons and delocalization at low losses. It is around 5 Å, down to <1 Å in ideal cases (STEM)**

Data treatment for chemical composition

data cube:

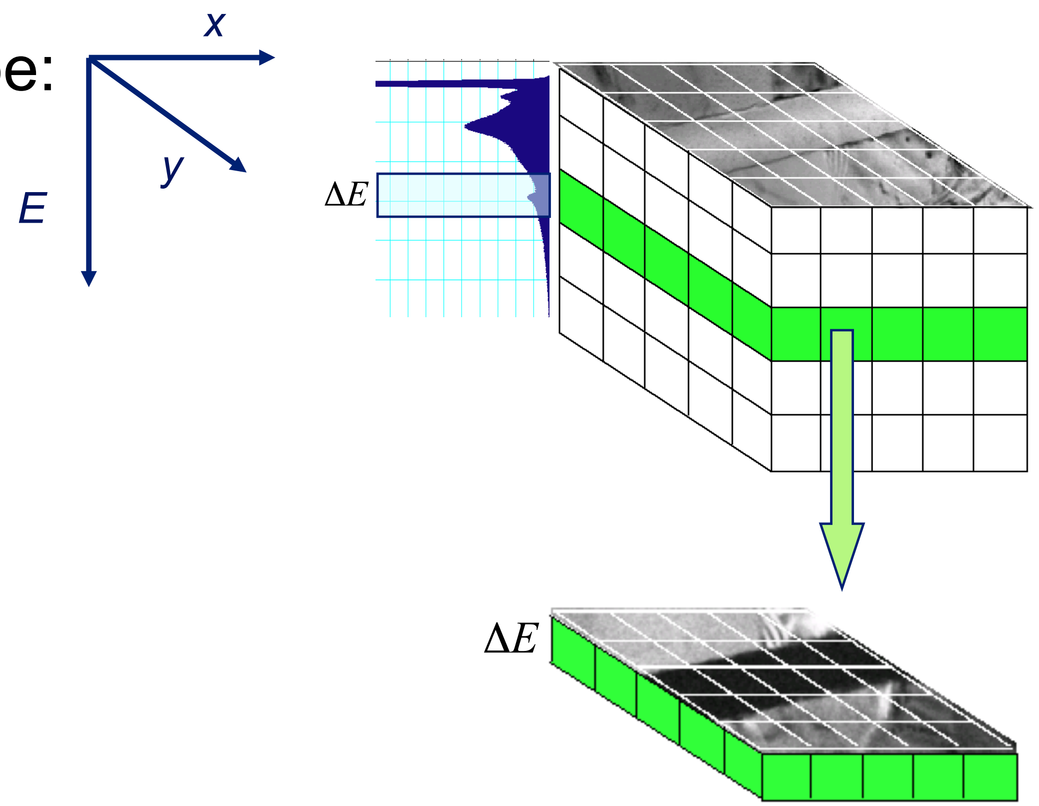

An energy filtered image $I(x, y, \Delta E)$ is a slice from the 3D data cube.

Data processing of data cubes using Multivariate Statistical Analysis (MSA):

- Recorded data suffers from imperfections, for instance from the presence of noise due to weak signal and/or to short acquisition times.
- Aim of data processing: enhance some parts of a composite signal at the expense of other (hopefully unwanted) parts.
- MSA looks for the directions in the variable space responsible for the maximum of variance and projects the dataset onto these.

F. Trebbia and N Bonnet, Ultramicroscopy 34 (1990) 165
E. R. Malinowski, Factor Analysis in Chemistry, 3rd Edition, Wiley Ed. 2002

A common MSA method: Principal Component Analysis (PCA)

PCA converts a dataset of correlated variables into another of uncorrelated (orthogonal) variables, called **principal components**.

Two-dimensional example

This axis explains most of the pixels dispersion: **component 1**

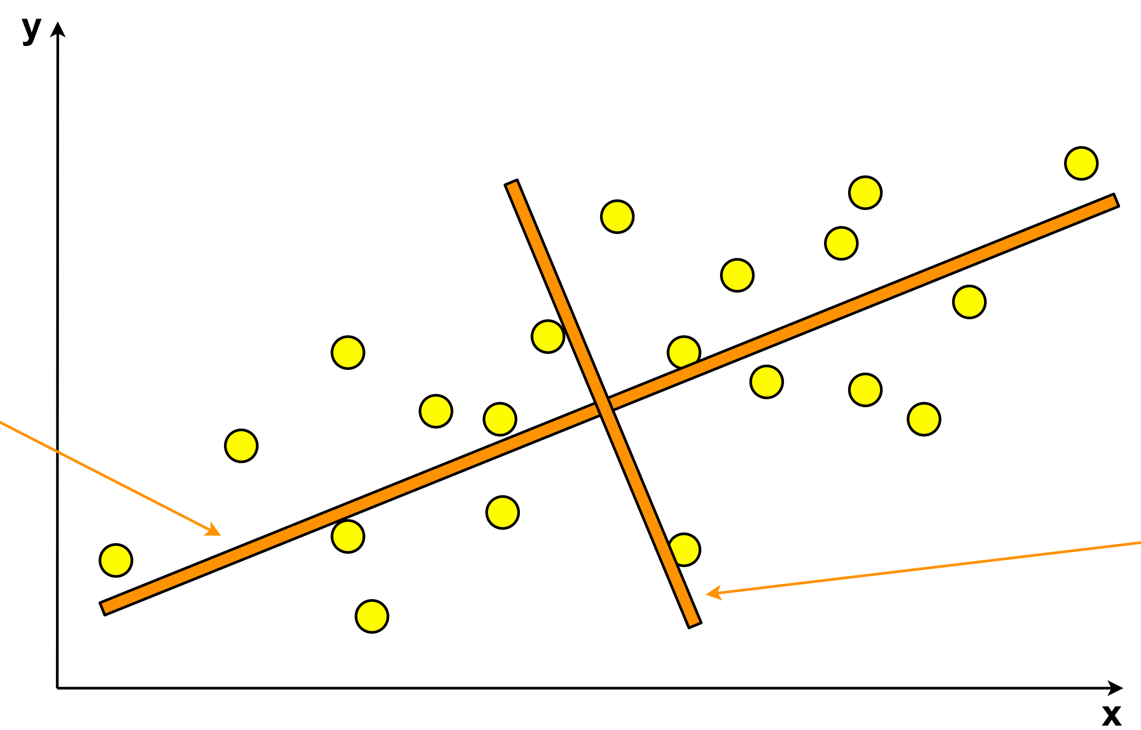

Second axis is perpendicular to the first one: **component 2**

PCA performs rotations on the original axes

- Axes of least variance can be disregarded to reconstruct the dataset

Model ODS ferritic steel: 83.4Fe, 14Cr, 2W 0.3Ti, $0.3Y_2O_3$, CRPP EPFL

Raw EFTEM data cube

Energy loss range: 350-760 eV

Microscope: TEM JEOL 2200FS
200 keV, FEG, in column filter
C. Hébert CIME EPFL

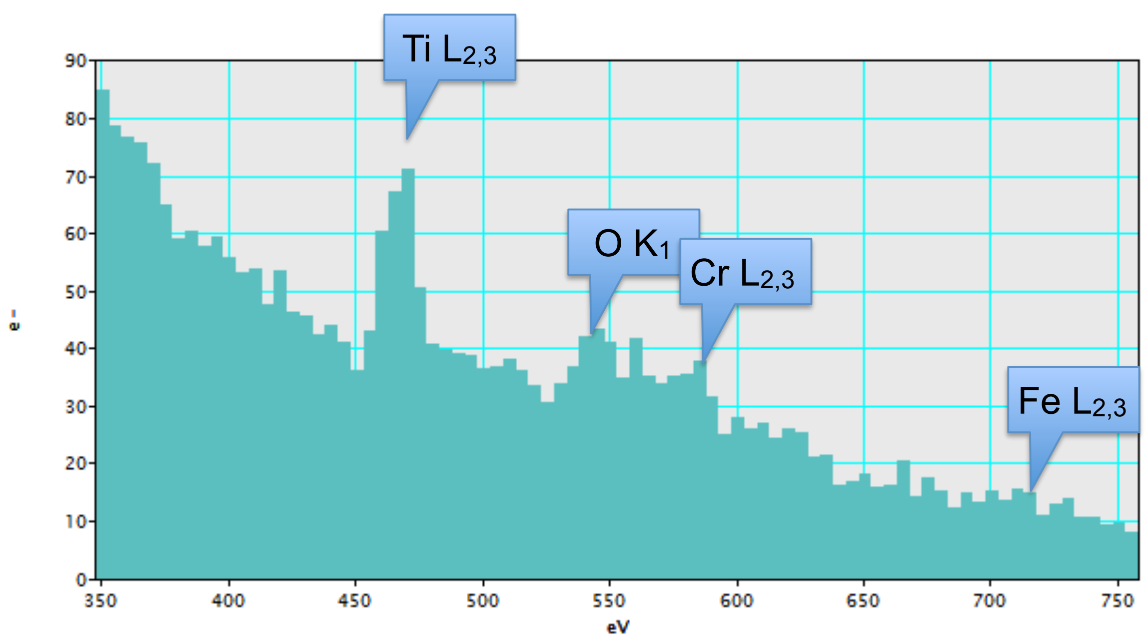

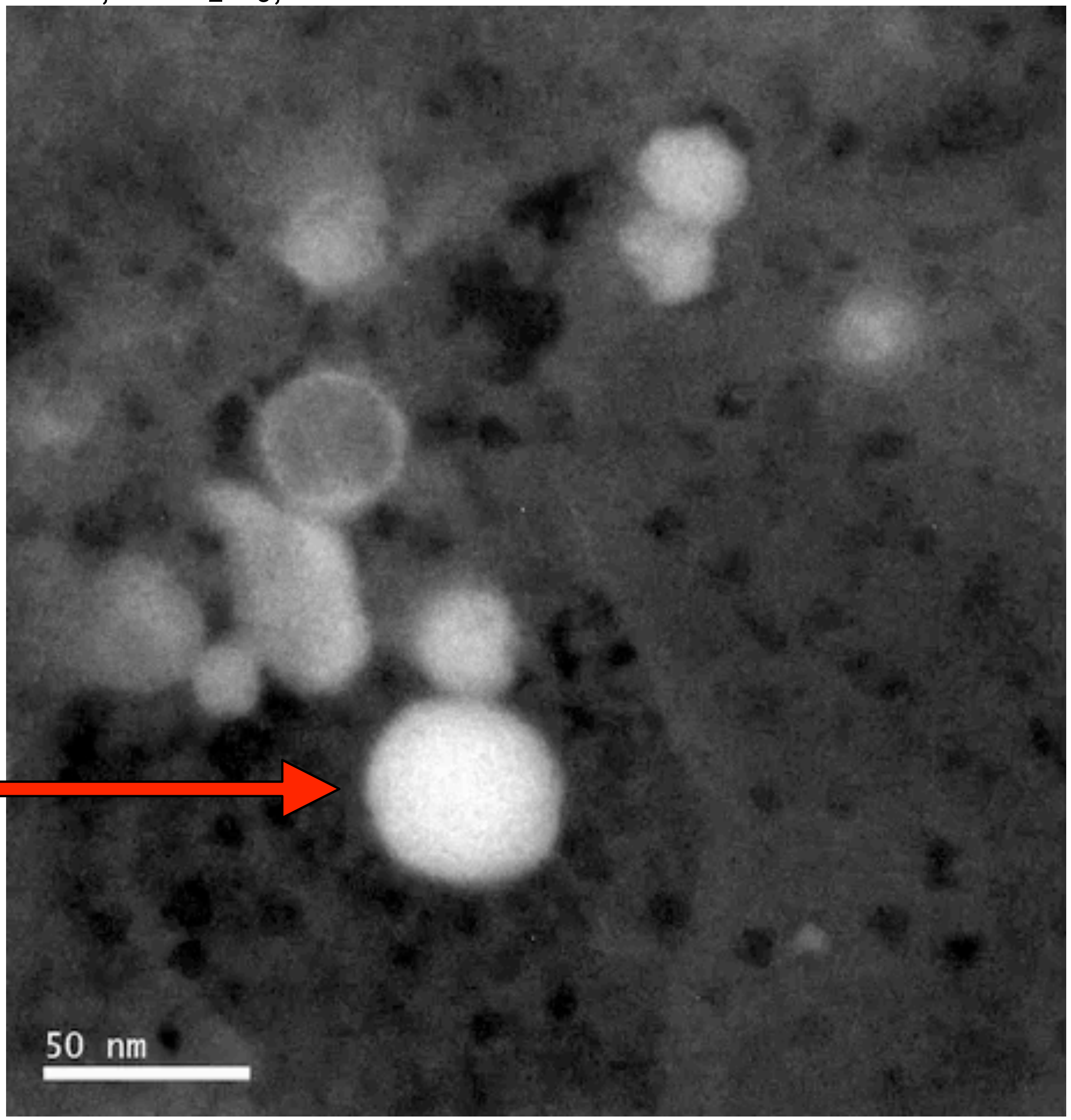

Movie showing images made with an energy loss sliding from 350 to 750 eV, 5 eV wide window

G. Lucas, CIME EPFL

PCA applied to data cubes obtained by EFTEM

PCA applied to EFTEM data cube

Energy loss range: 350-760 eV

Microscope: TEM JEOL 2200FS
200 keV, FEG, in column filter

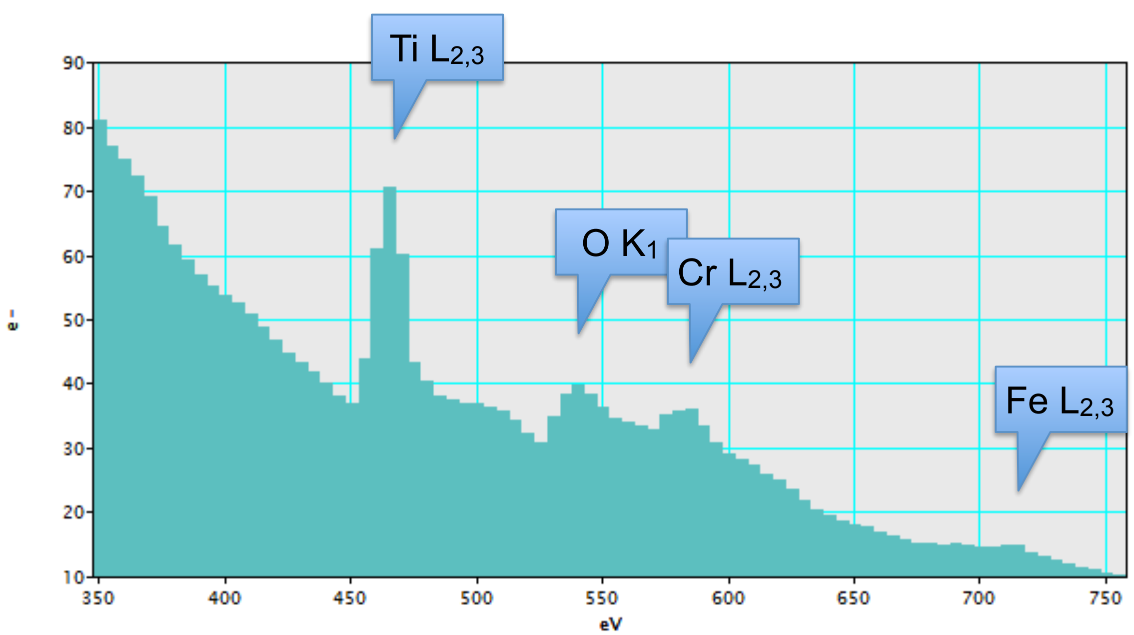

Model ODS ferritic steel: 83.4Fe, 14Cr, 2W 0.3Ti, 0.3Y_2O_3, CRPP EPFL

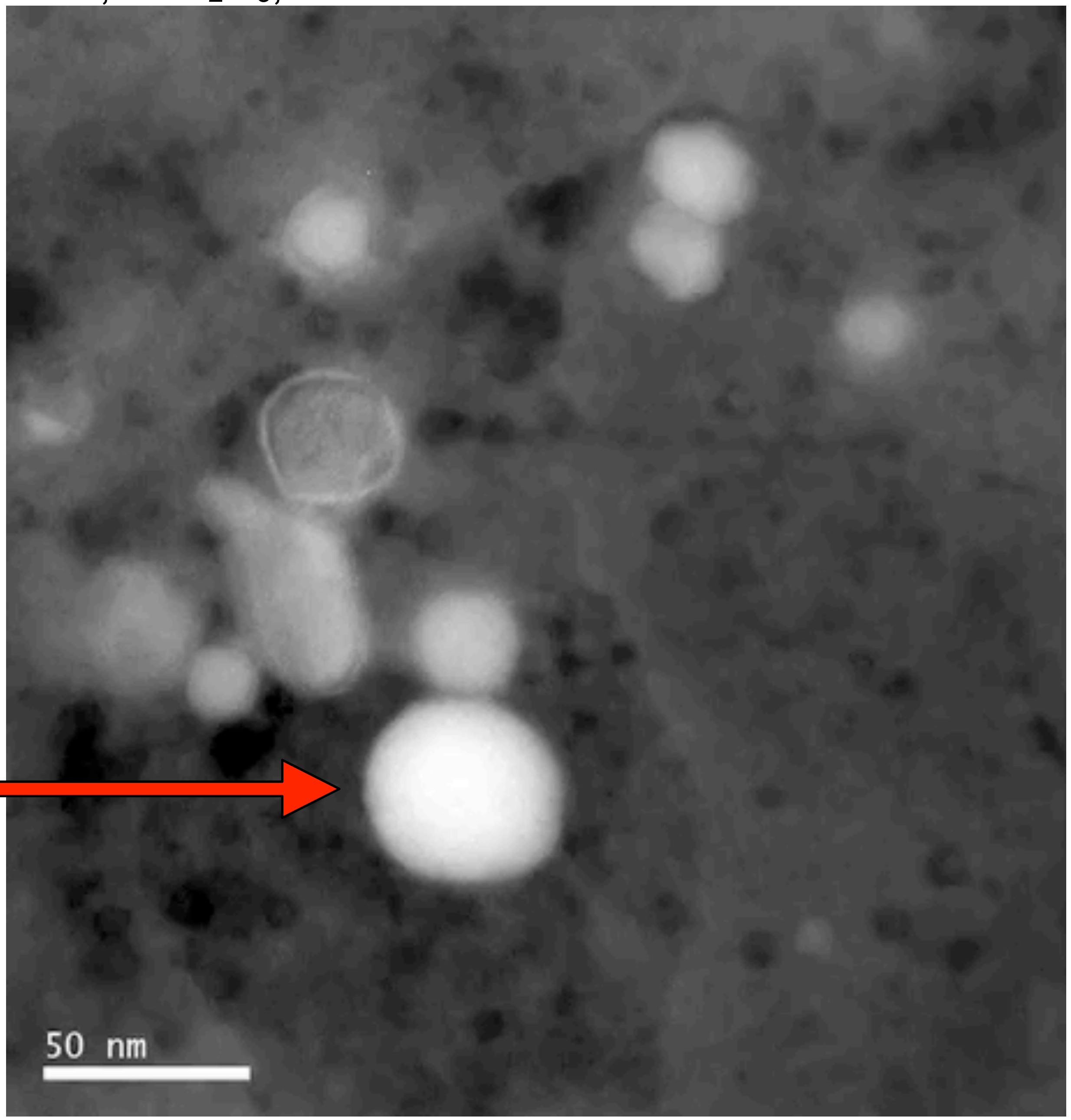

Movie showing images made with an energy loss sliding from 350 to 750 eV, 5 eV wide window

• with PCA, spectrum quality is largely improved

PCA applied to data cubes obtained by EFTEM

Model ODS ferritic steel: 83.4Fe, 14Cr, 2W
0.3Ti, 0.3Y_2O_3, CRPP EPFL

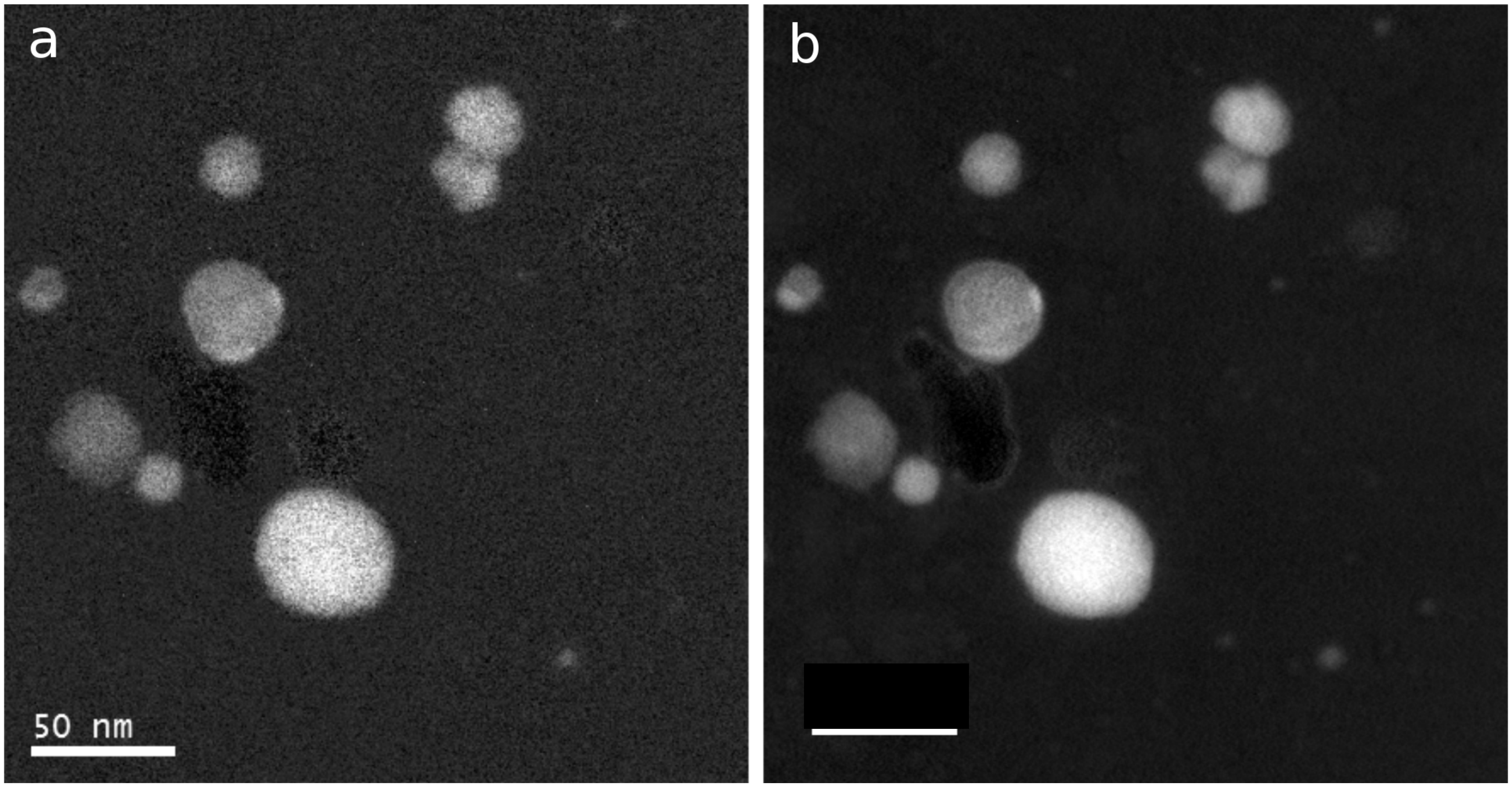

Elemental map performed on titanium L_3 (456 eV) and L_2 (462 eV) edges
a) without PCA, background removal is problematic and leads to noise
b) with PCA, image quality is largely improved
notice e.g. the shell structure in the particle above the black feature

PCA applied to data cubes obtained by EFTEM

Model ODS ferritic steel: 83.4Fe, 14Cr, 2W 0.3Ti, 0.3Y_2O_3, CRPP EPFL

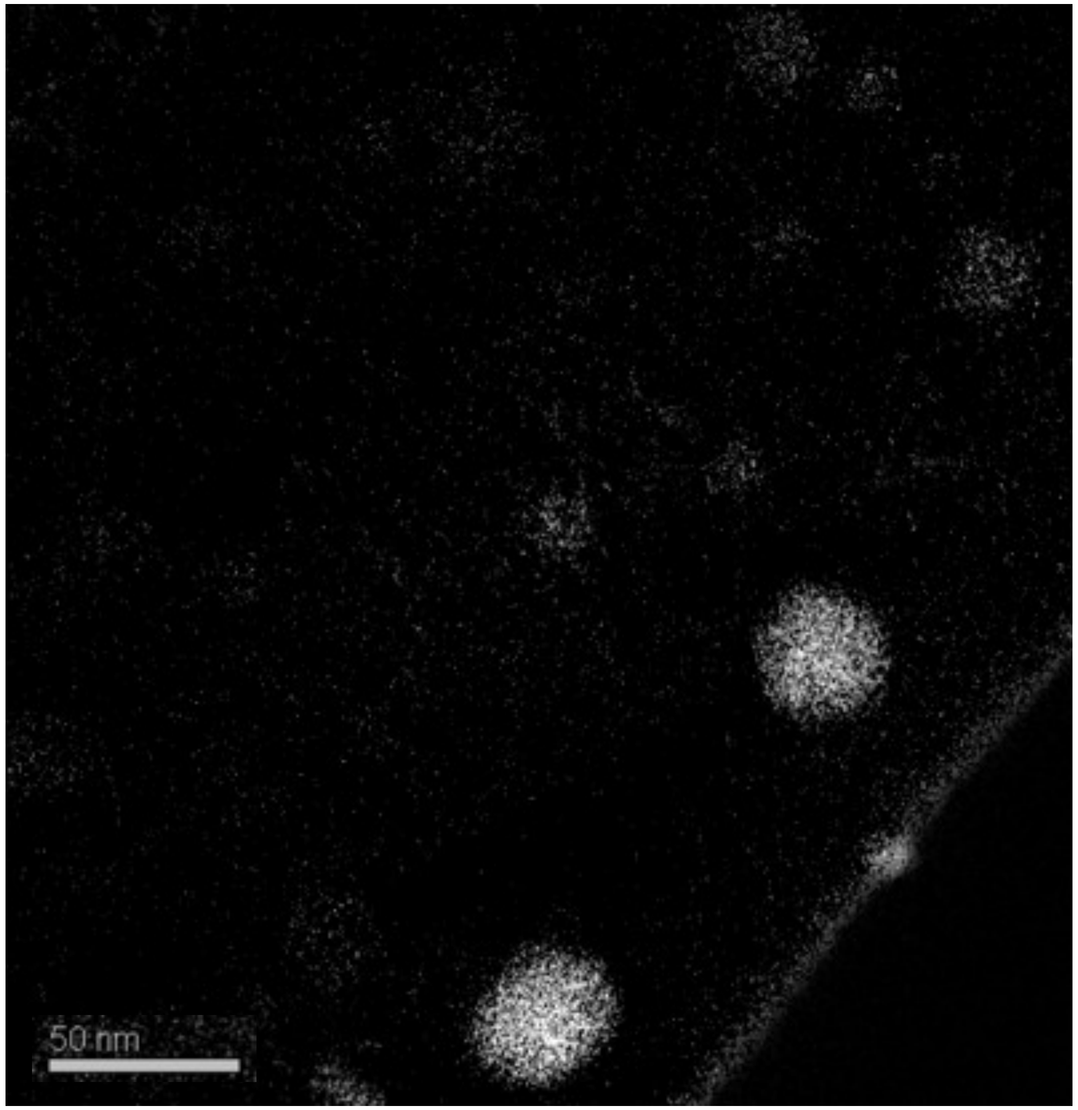

Raw data, energy loss window: 29.8-39.8 eV

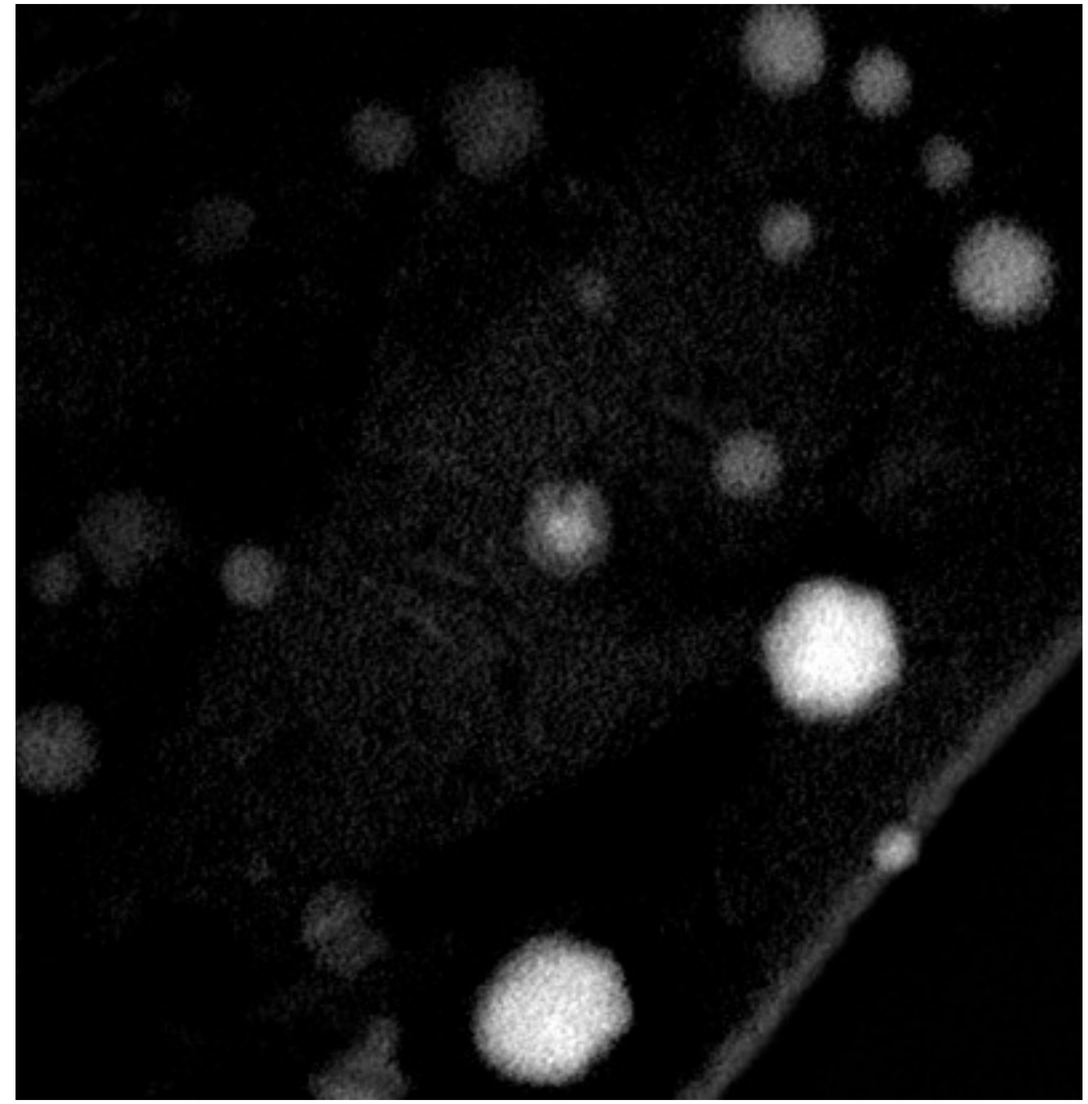

PCA treated data, energy loss window: 29.8-39.8 eV

- again, with PCA, image quality is largely improved

notice the revealed smallest particles, the facets of the largest particles and the shell structure of the particle in the middle

In principle PCA applies to any other type of data, such as STEM X-ray EDS or EELS maps

TEM tomography

3D reconstruction of dislocation structure in Al induced by deformation

141 pictures taken every degree from -70° to +70°
double tilt rotation holder
TEM FEI Tecnai 200 kV
bright field

Dr. Amuthan Ramar
CEN DTU Denmark

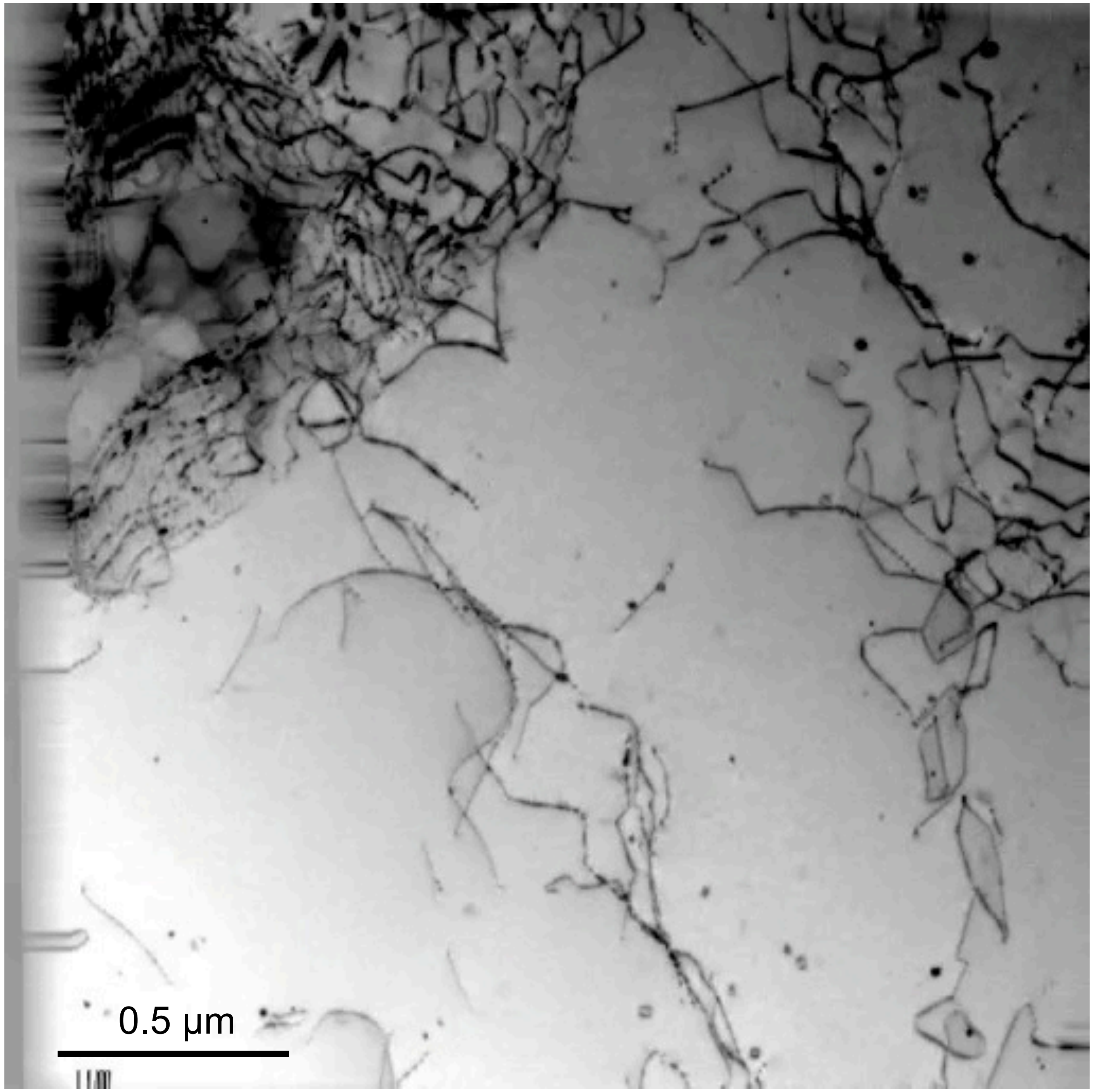

TEM tomography

3D reconstruction of dislocation structure in Al induced by deformation

141 pictures taken every degree
from -70° to +70°
double tilt rotation holder
TEM FEI Tecnai 200 kV
bright field

Dr. Amuthan Ramar
CEN DTU Denmark

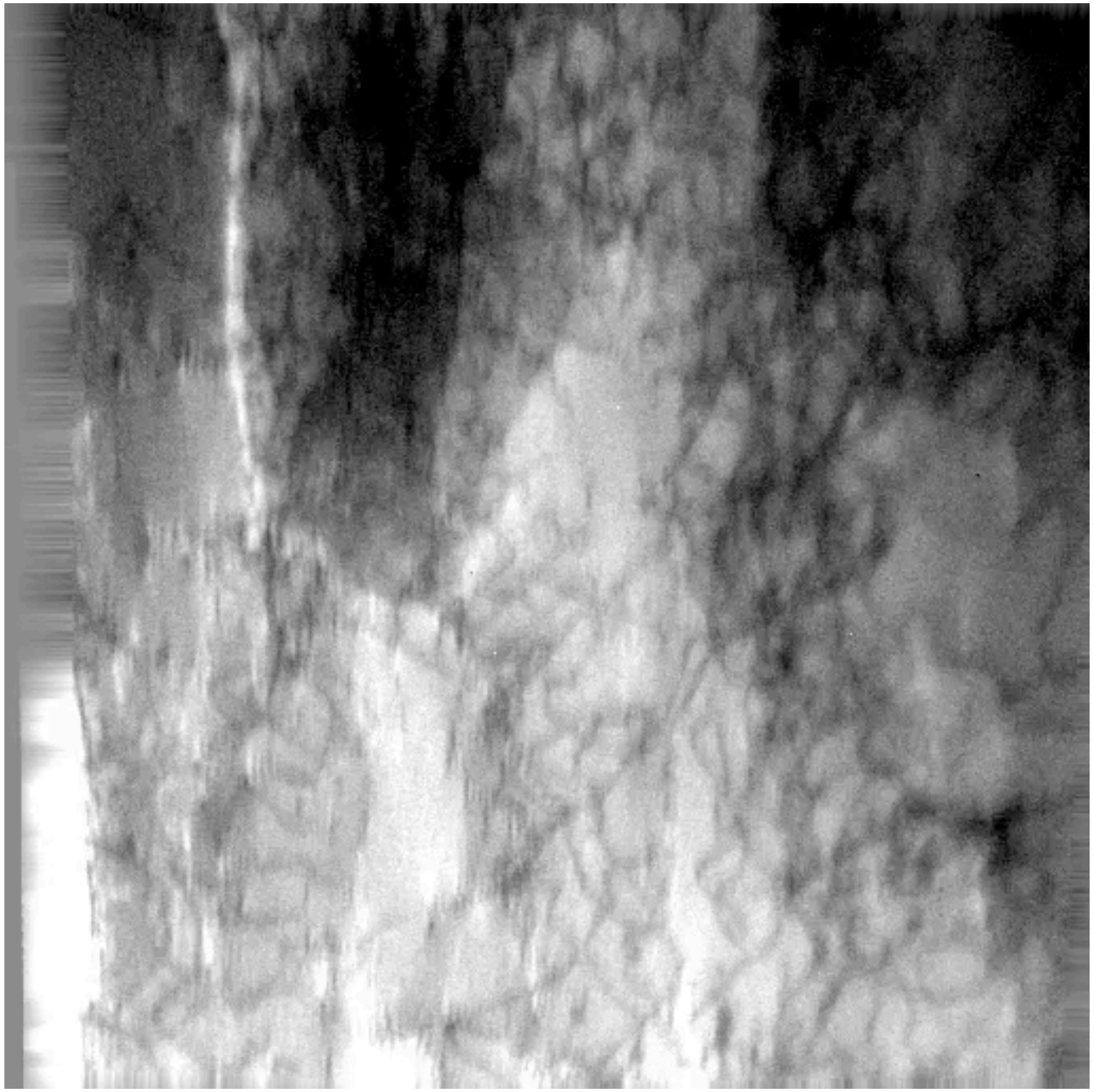

- **Tomography in TEM allows raising ambiguities due to the 2D projection of a 3D object**

TEM tomography

3D reconstruction of dislocation structure in Al induced by 20% deformation

141 pictures taken every degree
from -70° to +70°
HATA® double tilt rotation holder
STEM FEI® analytical TITAN 200 kV
UHAADF detector

Dr. Amuthan Ramar
CEN DTU Denmark

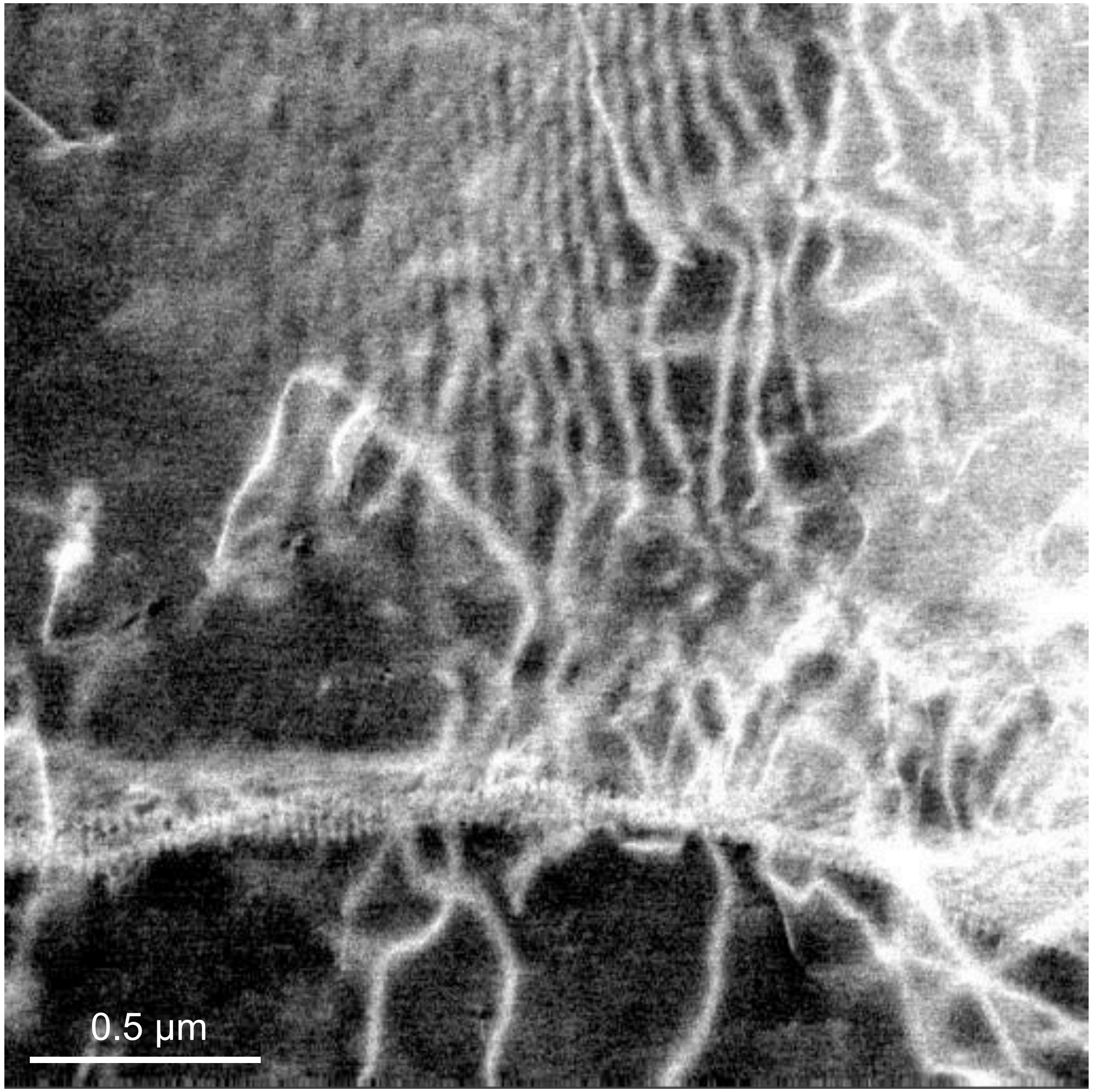

- **Tomography in TEM allows raising ambiguities due to the 2D projection of a 3D object**

TEM tomography

3D reconstruction of dislocation structure in Al induced by 20% deformation

141 pictures taken every degree from -70° to +70°
HATA® double tilt rotation holder
STEM FEI® analytical TITAN 200 kV
UHAADF detector

Dr. Amuthan Ramar
CEN DTU Denmark

- **Tomography in TEM allows raising ambiguities due to the 2D projection of a 3D object**

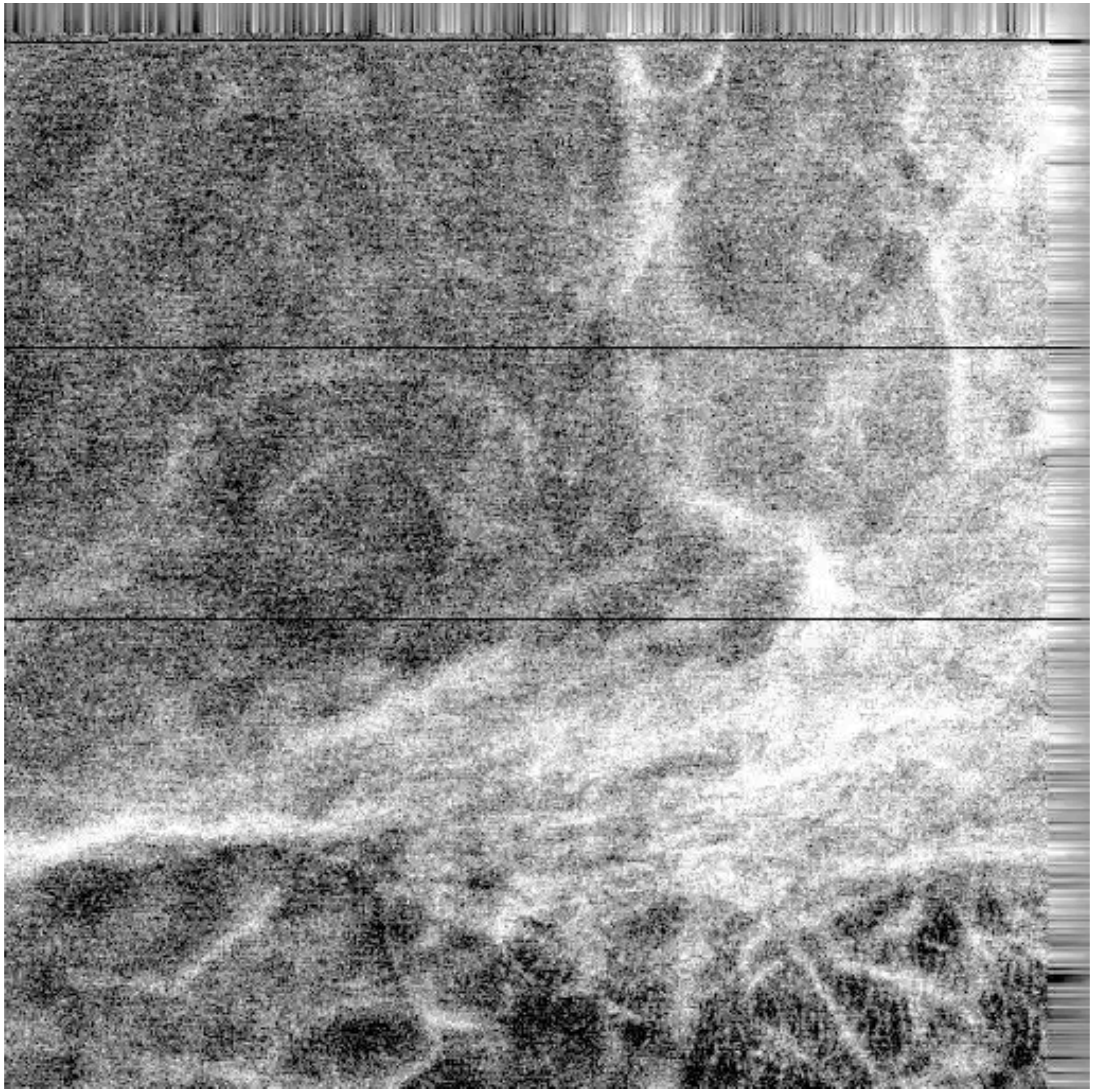

TEM in situ experiments

JANNuS experiment

B. Décamps, O. Kaïtasov
CNRS Orsay

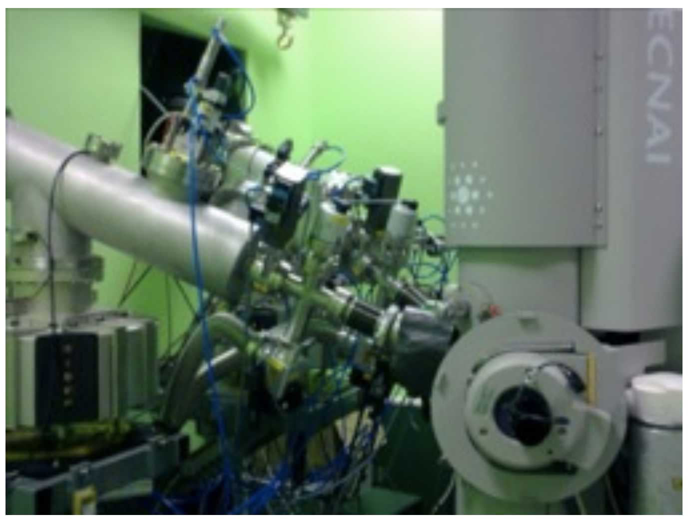

Experiments performed on ultra high purity ferritic materials in view of validating modelling of radiation damage

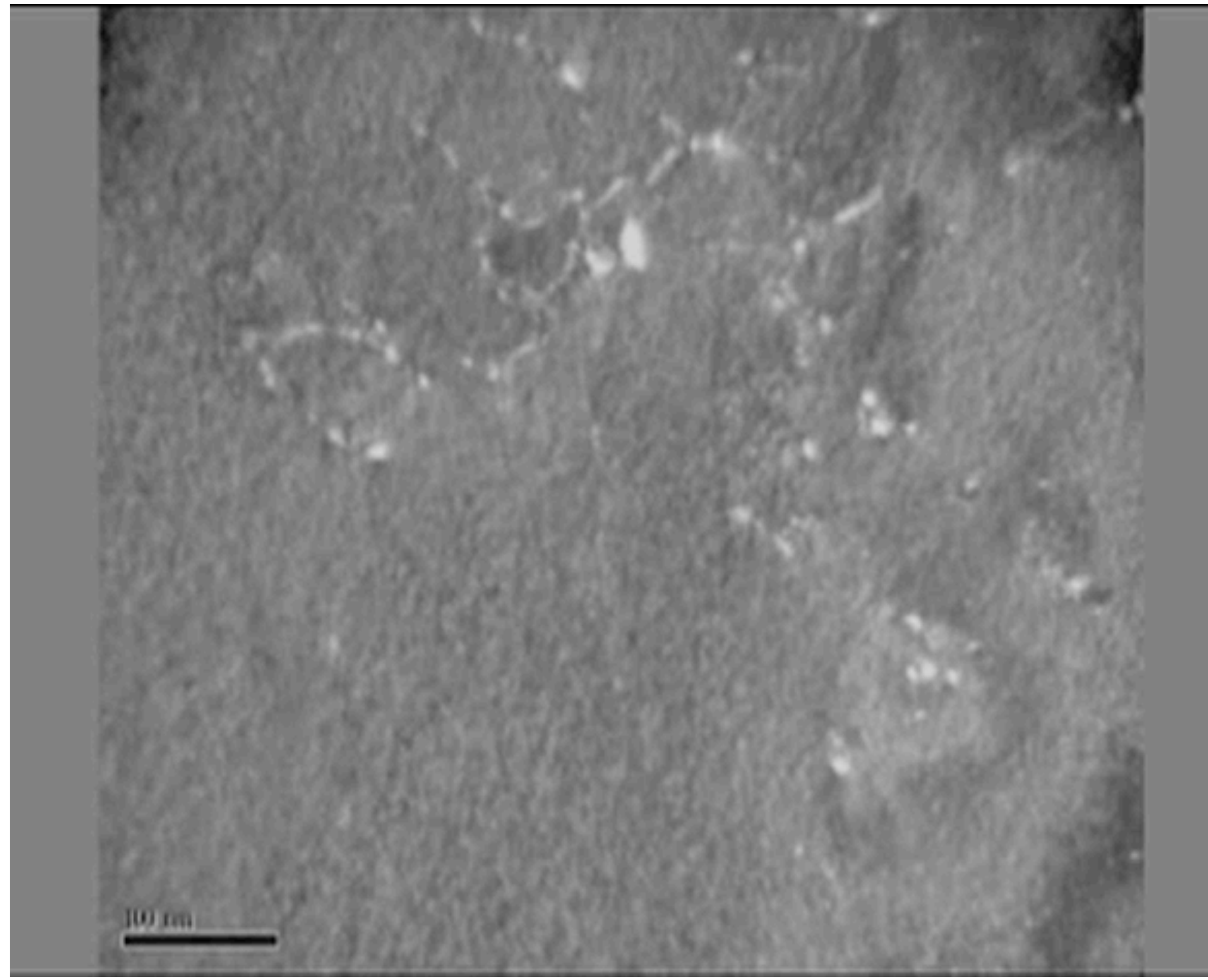

Single beam Fe 300 KeV, 1 dpa, RT, on UHP Fe, CRPP
Movie accelerated 50x
TEM observation condition 200 kV WBDF g(4g) g(110)

ex situ ION IRRADIATION/IMPLANTATION, JANNUS SACLAY

UHP Fe CRPP irradiated at RT to
1 dpa with 24 MeV Fe^{8+}
1000 appm He with 2 MeV He^{+}

Y. Serruys, P. Trocellier CEA Saclay

TEM prepared by FIB at WUT
+ ‘gentle ion mill’

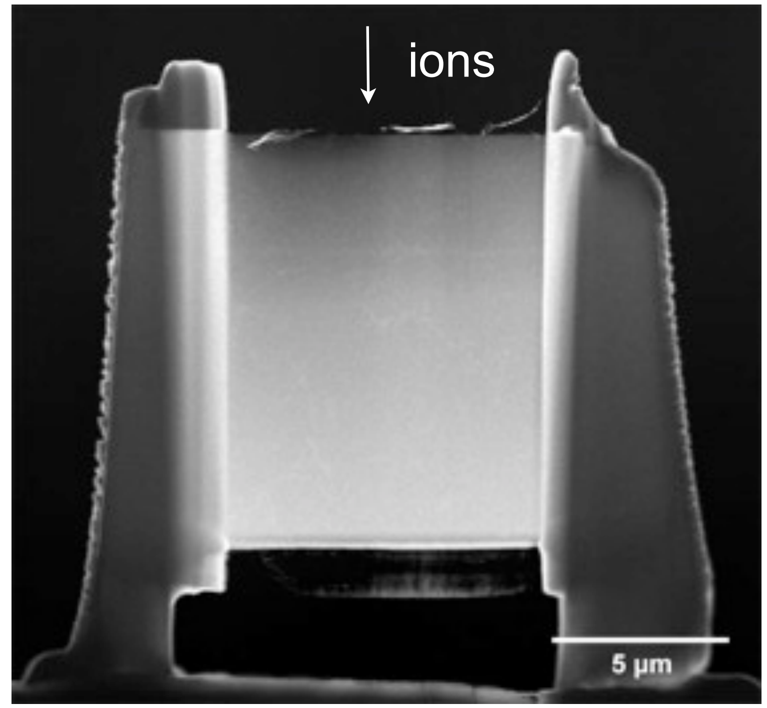

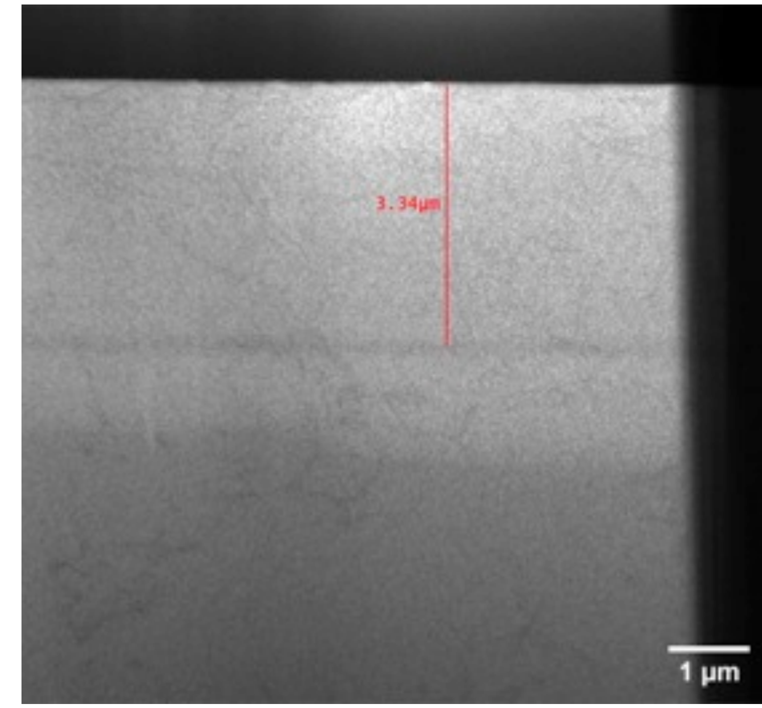

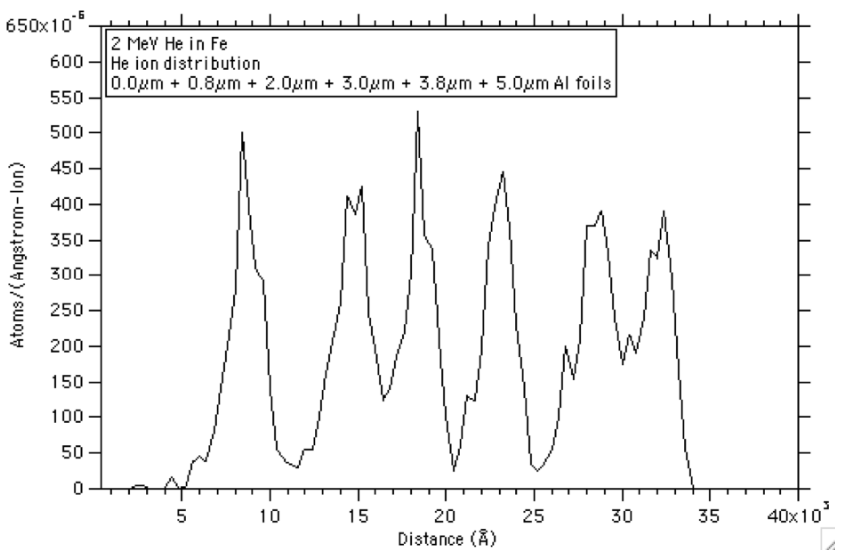

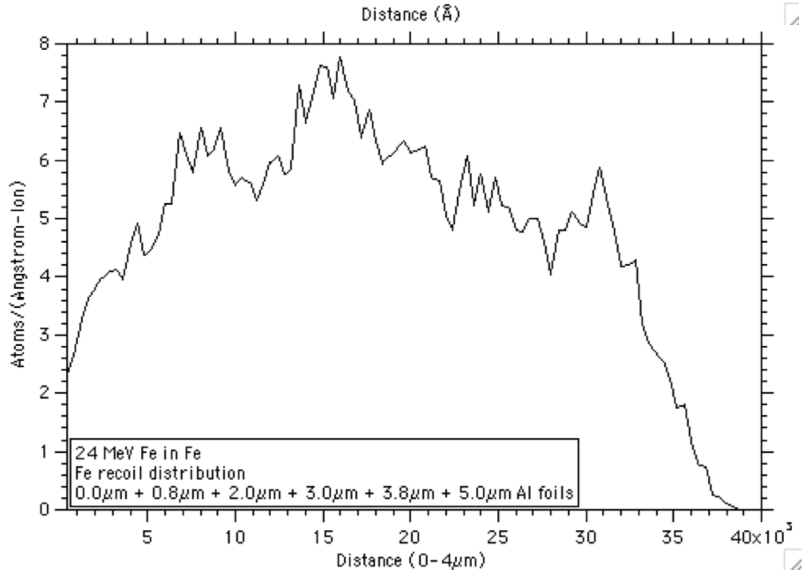

surface

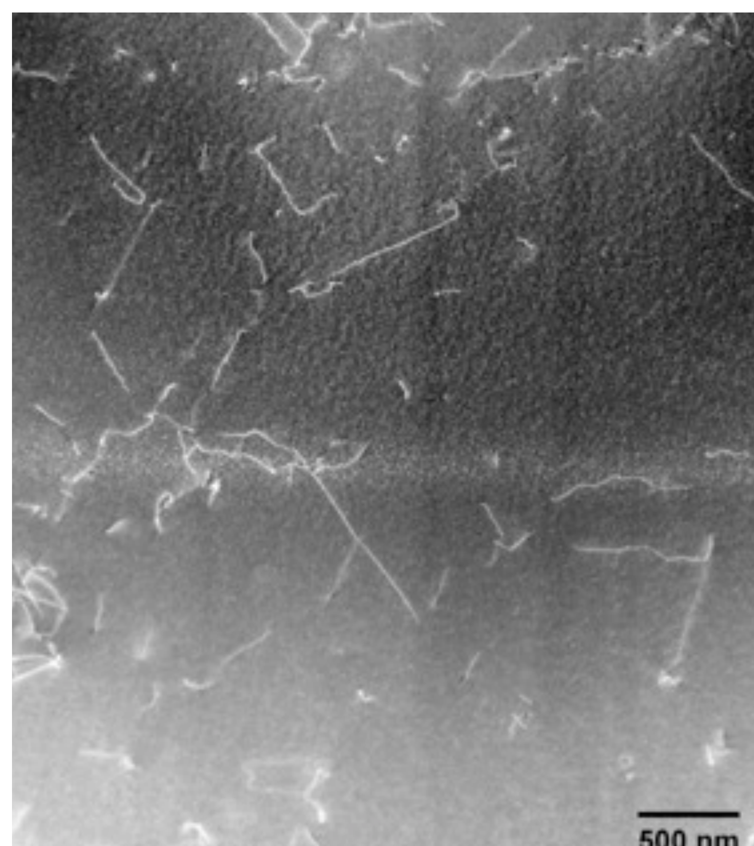

implanted region

low defects density

T. Plocinski, Warsaw University of Technology

ex situ ION IRRADIATION/IMPLANTATION, JANNUS SACLAY

TEM sample preparation technique problem with the FIB: it creates radiation damage !

FLASH POLISHING

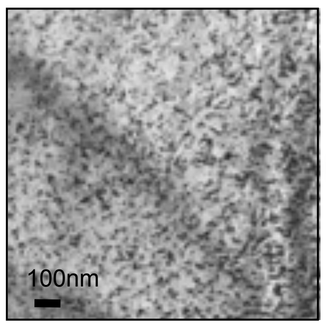

FIB'ed sample: W-2Y_2O_3

Dimensions: 5x10 μm

Thickness: 150 nm

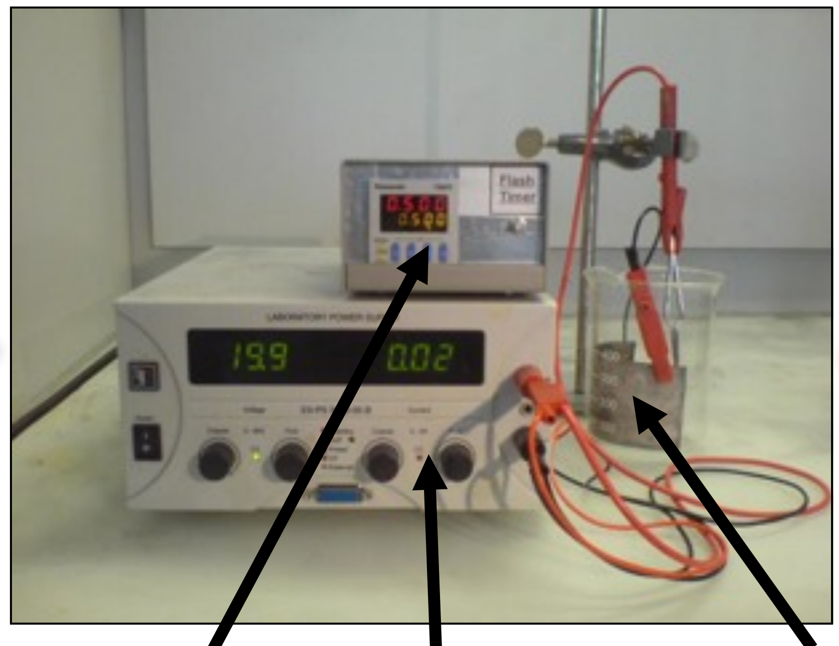

Flash timing
1ms resolution

Power Supply
20 V, ~0.1 A

NaOH solution
RT

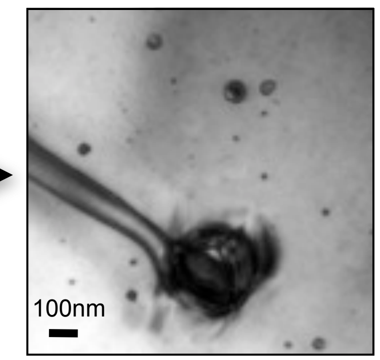

TEM lamella after FIB and flash polishing

L. Veleva, R. Schäublin, A.Ramar, Z. Oksiuta, N. Baluc European Microscopy Congress 2008, Volume 2: Materials Science, Eds. S. Richter and A. Schwedt, Springer-Verlag Publication, Berlin Heidelberg, Germany, (2008) 503-504

- Flash polishing allows removing the radiation damage induced by the Focused Ion Beam preparation.
- TEM reveals the oxide particles embedded in the W matrix.

Other possibility: gentle ion mill = lower energy Ga ions (<2 keV) for the final polishing
Could be a solution, depending on the level of details required (5 nm or below)

TEM in situ experiments

In situ heating experiments

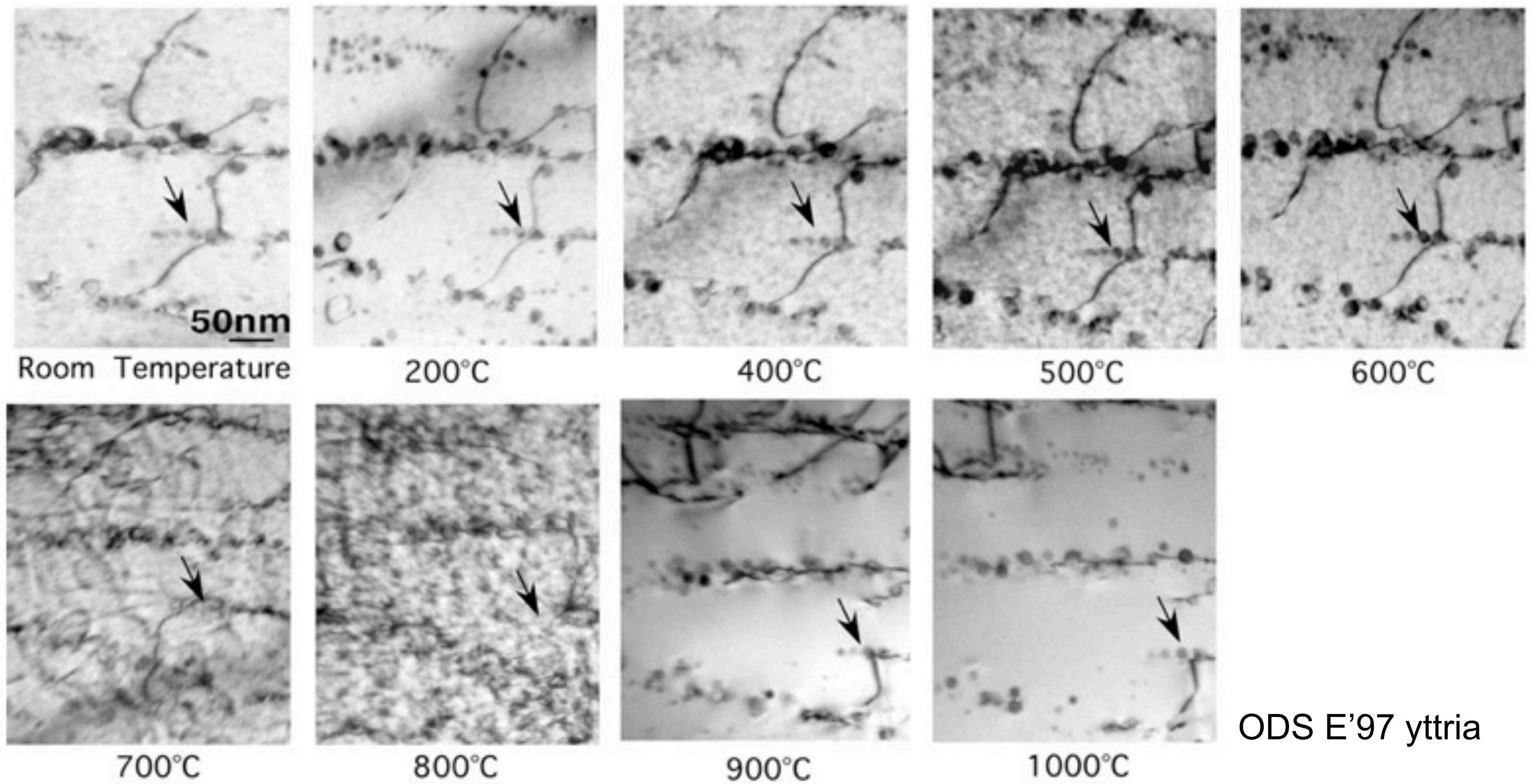

ODS E'97 yttria

Thermal stability of Y_2O_3 oxides in ODS EUROFER97
How about the stability of Y-Ti-O oxides ?

A. Ramar CRPP / V. de Castro, U. Carlos III, Madrid / U. of Oxford

TEM in situ experiments

In situ heating experiments

ODS E'97 yttria + Ti

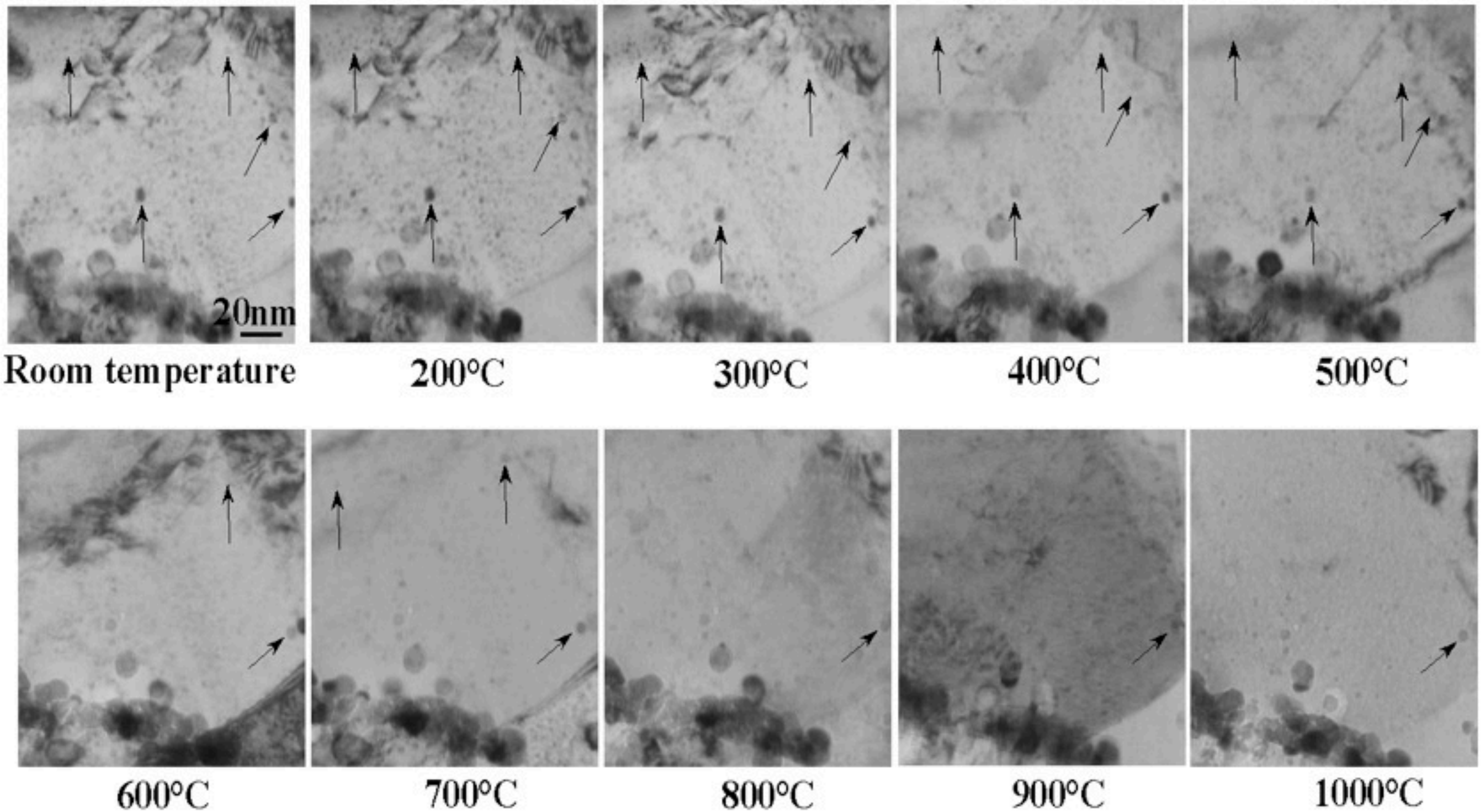

Thermal stability of Y-Ti-O oxides remains an open question

A. Ramar CRPP / V. de Castro, U. Carlos III, Madrid / U. of Oxford

TEM image simulations

Single beam 500 keV Fe, 1 dpa, RT

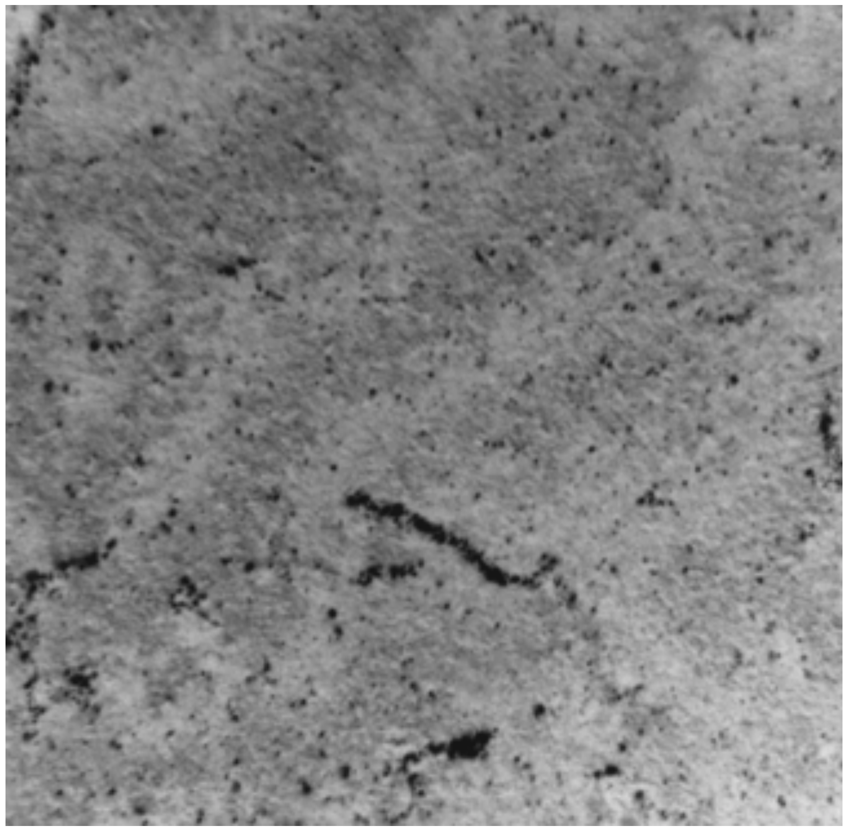

Dual beam 500 keV Fe, 1 dpa,10 keV He, 0.1 $^{a}/_{o}$,

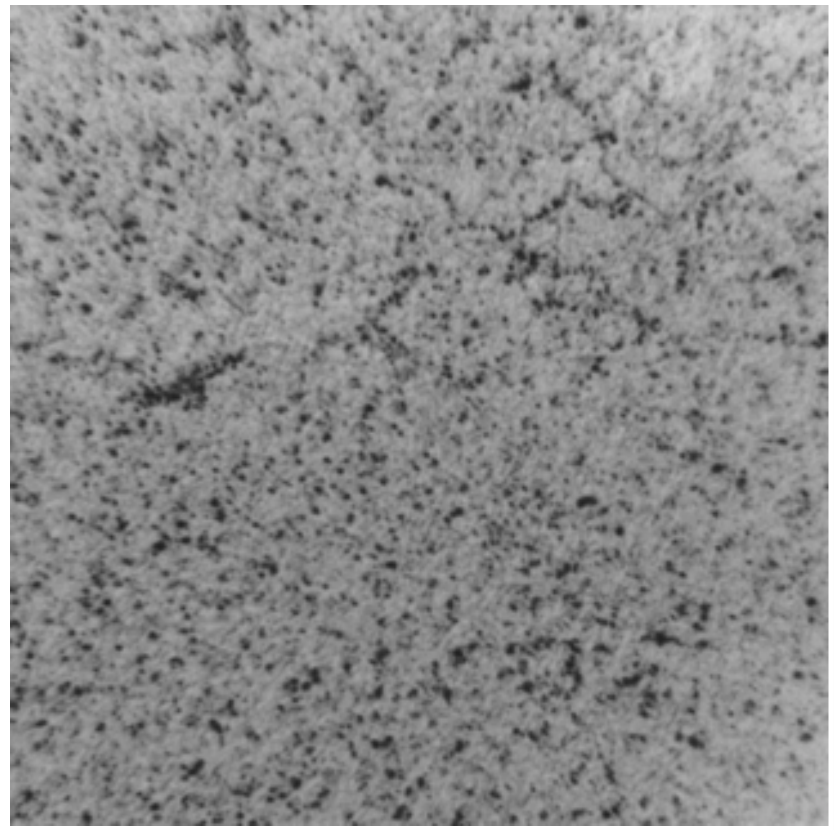

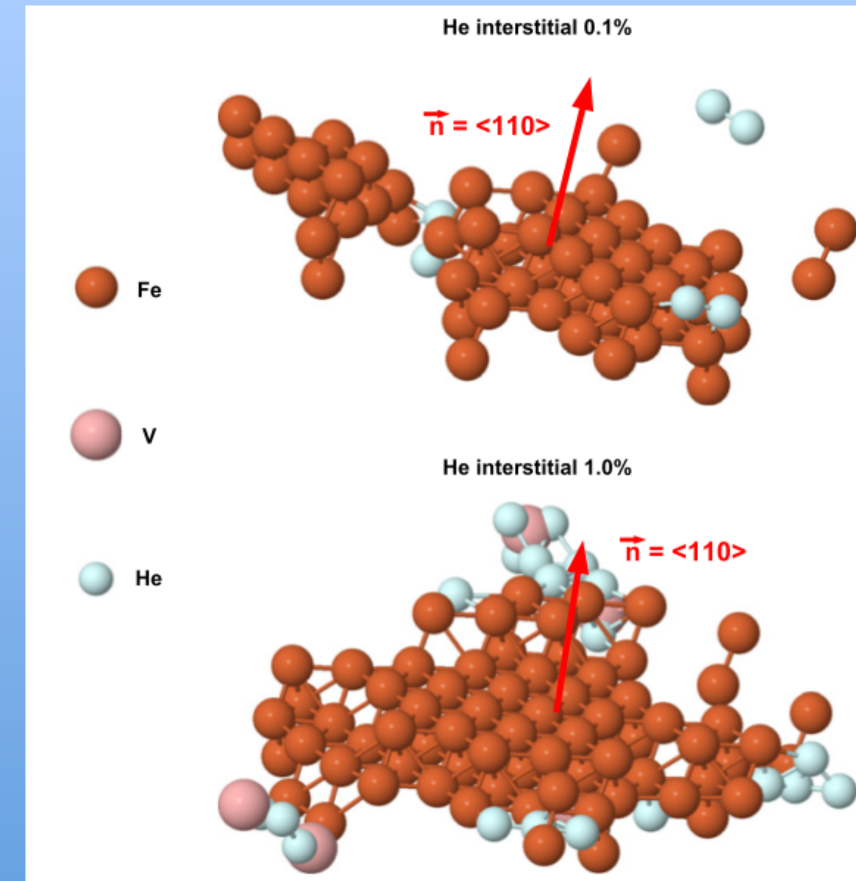

- Number and size of SIA clusters increase with He_{int} content
- **He Stabilizes SIA clusters**

G. Lucas, R. Schäublin, Helium effects on displacement cascades in α-iron, J. Phys.: Condens. Matter 20 (2008) 415206

- Preliminary results show large effect of He on the primary damage in Fe
- Interesting correlation with MD simulation
- Very promising experiments in view

How to validate molecular dynamics simulation results ?
... TEM image simulation

Stacking fault
tetrahedra in
irradiated copper

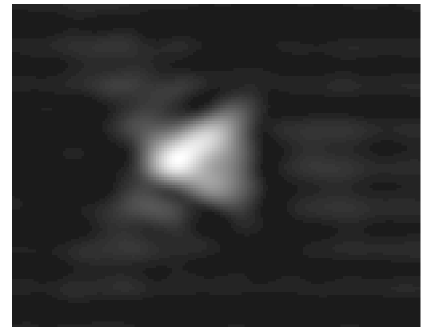

Multislice TEM image simulation

Experiments

Simulations

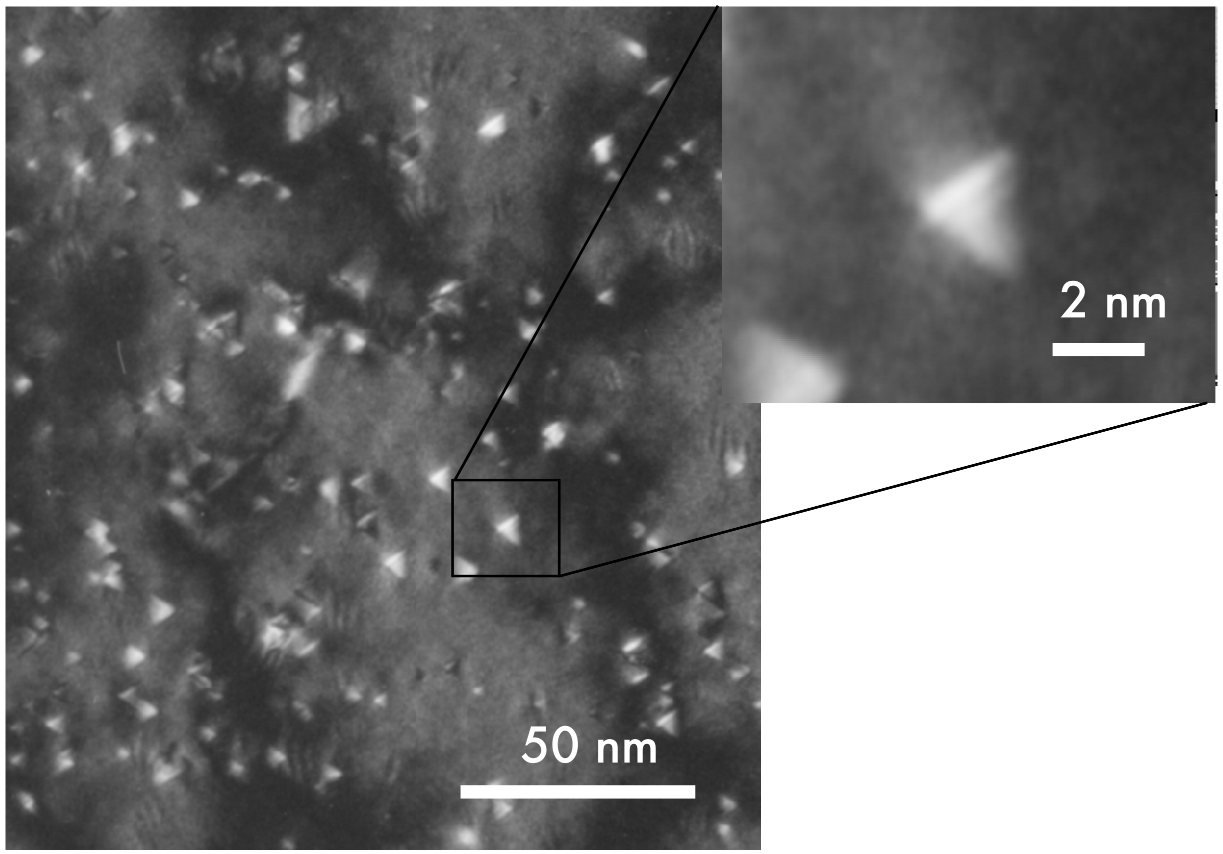

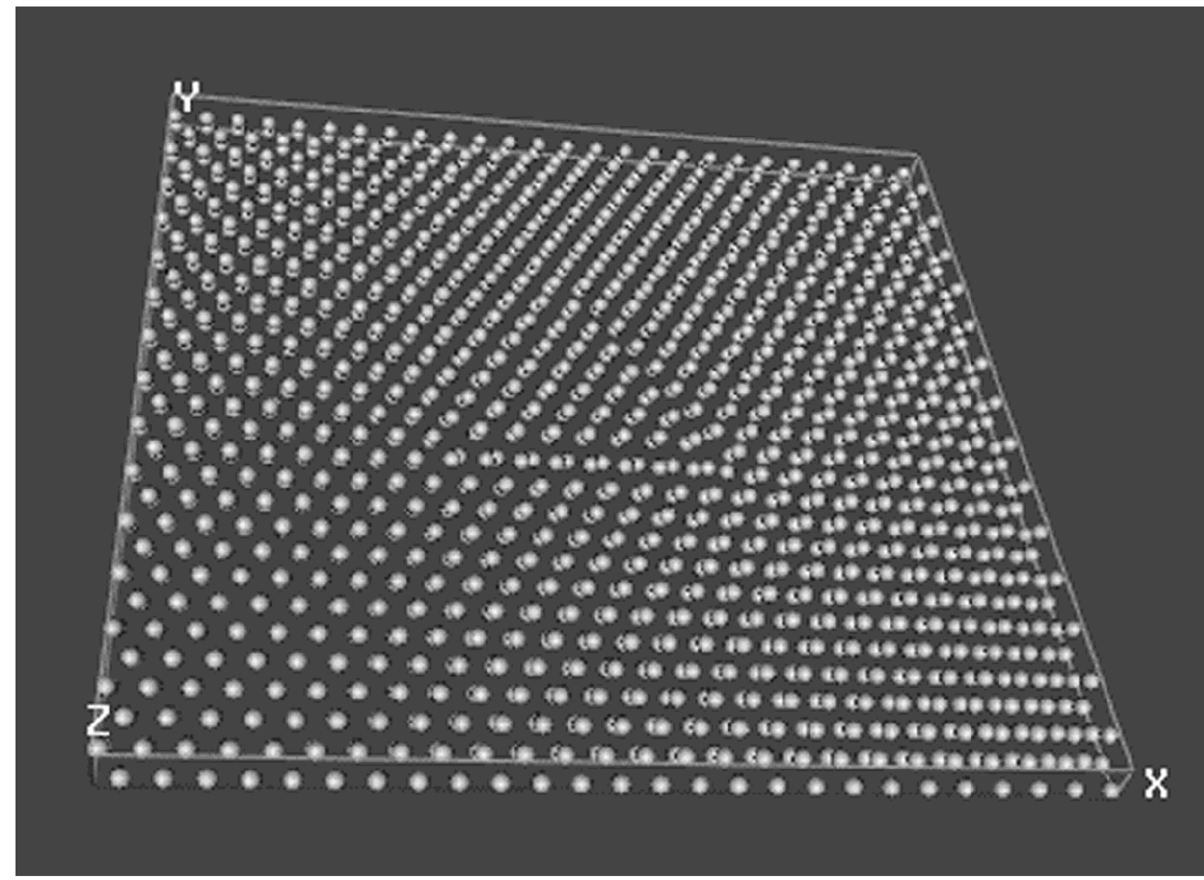

Cu 0.01 dpa RT
TEM weak beam g(6g) g = (200)

Molecular dynamics simulation
Pair potential method, 100’000 atoms

R. Schäublin, Y. Dai, Y. Osetsky, M. Victoria Institute of Physics Publ. (1998) 173-174

TEM image simulation allows validating MD simulation

on going work with D. Terentyev SCK·CEN Mol on GB in Fe and E. Meslin CEA Saclay
on dislocation loops in ferritic material

TEM image simulations

outlook: 4D TEM

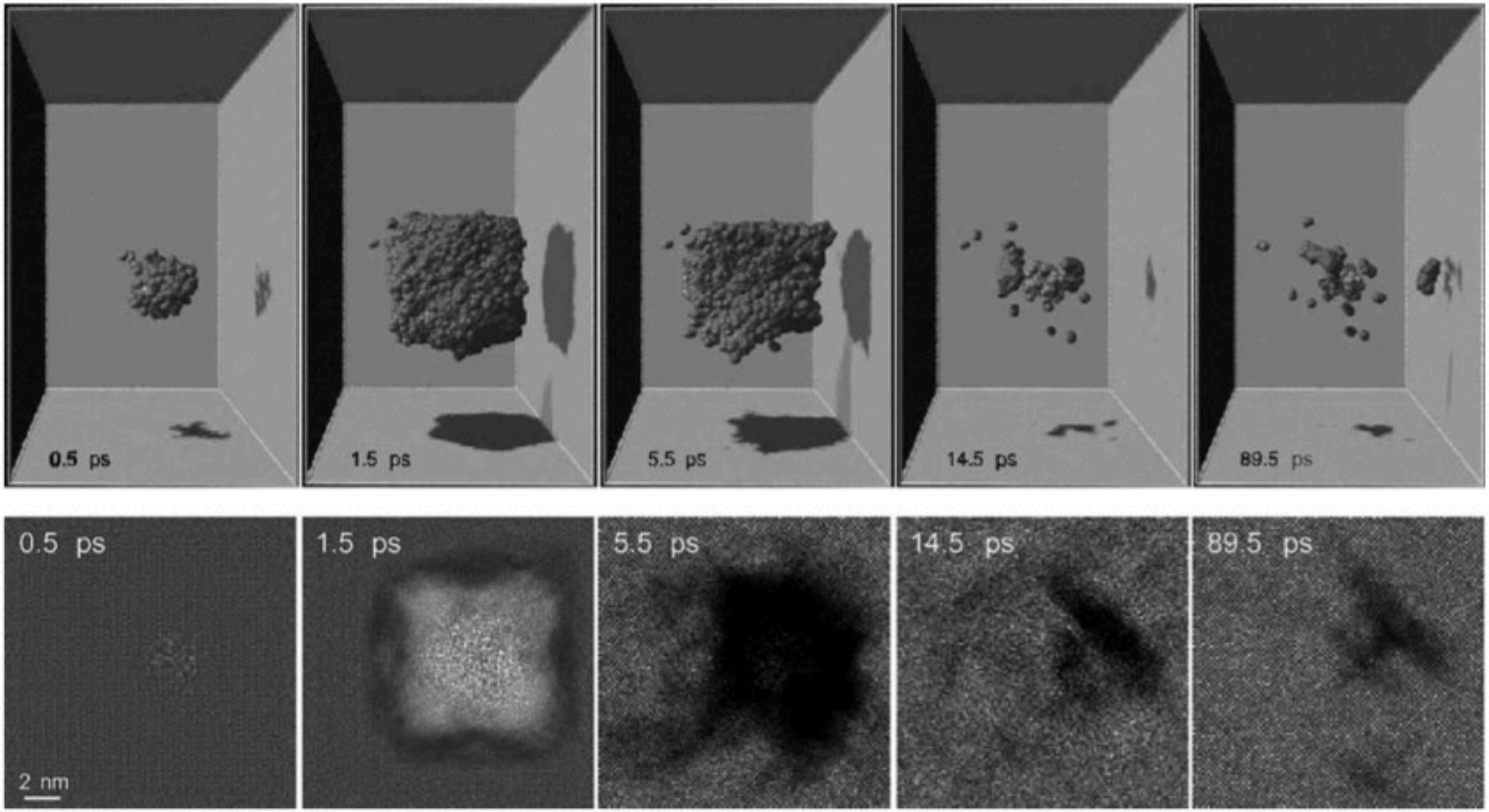

Cu 20 keV cascade time evolution (MD + TEM image simulation)
R. Schaeublin, M.-J. Caturla, M. Wall, T. Felter, M. Fluss, B.D. Wirth, T. Diaz de la Rubia M. Victoria Journal of Nuclear Materials 307–311 (2002) 988–992

> DTEM to experimentally observe the displacement cascade

Conclusions

• Recent advance in TEM techniques is a large benefit for the development of materials for fusion (steels, ODS steels, ODS W, ...)

Cs corrected STEM imaging and chemical mapping
Energy filtered TEM
High angle dark field STEM imaging
Tomography
...
TEM in situ experiments:
Ion implantation at JANNuS, unique in the world
heating and straining

Data analysis, TEM image simulations

• Collaborative work across Europe is essential as the cost of acquisition and use of such equipments becomes prohibitive for a single lab

CRPP
ÉCOLE POLYTECHNIQUE FÉDÉRALE DE LAUSANNE